Understanding the Q^2 discrepancy in the $CC\pi^+$ sample

Rein-Sehgal model improvements: muon mass and form factors

William Metcalf and Jarosław Nowak

Louisiana State University

August 25, 2008

BooNE Technical Note 260

Contents

I Introduction

In new experiments such as K2K or MiniBooNE it has been observed that the description of cross section of neutrino interaction as a function of Q^2 is not sufficient, i.e. observed number of events is lower for low Q^2 and higher for rest of the predicted distribution. There is no simple explanation for this phenomenon. We should rather assume that with new experiments we reach a precision for which we can and ought to bring our Monte Carlo generators up to date. The K2K collaboration revisited the charged-current coherent pion production, concluding that it was overestimated and set a upper limit of its contribution to the inclusive charged-current interactions to 0.60×10^{-2} [7] . The MiniBooNE experiment in the results for $CCQE$ interaction on carbon set an effective value of axial-vector mass to $M_A^{eff} = 1.23 \pm 0.20 GeV$, and introduced an effective parameter $\kappa = 1.019 \pm 0.011$, which modifies the Pauli-suppression and reduces the discrepancy between data and Monte Carlo prediction [1].

In the neutrino-induced $CC\pi^+$ production the MiniBooNE experiment sees the suppression in the low Q^2 region. In figure 1 predictions of the reconstructed Q^2 and neutrino energy distributions for $CC\pi^+$ samples in neutrino mode are shown. It is clear that the description is not sufficient.

The discrepancy for Q^2 for the $CC\pi^+$ sample shown in figure 1 is a long standing problem and the main goal of this paper is to understand it better. In the first step we will modify the Rein-Sehgal model [8] of resonant pion production to include muon mass effect and new forms of form factors. With new model of pion production we will make an attempts to fit a axial mass for pion production and a contribution of the coherent production.

The prediction of neutrino interactions in the MiniBooNE experiment is based on customized for carbon nucleus Monte Carlo generator Nuance v3. In the Nuance generator the resonance $CC\pi^+$ production is describe by the Rein-Sehgal model (RS)[8]. The Rein-Sehgal model in based on the FKR model [3] and it describes pion production by excitation of 18 resonances with a cut at $W = 2\ GeV$ in hadronic invariant mass. The resonance production is described in terms of helicity amplitudes and cross section contains a interference terms and nonresonant background as well. The vector and axial-vector form factors have similar form like in the case of quasi-elastic scattering, but there is additional factor connected with the resonances. Each of the form factors

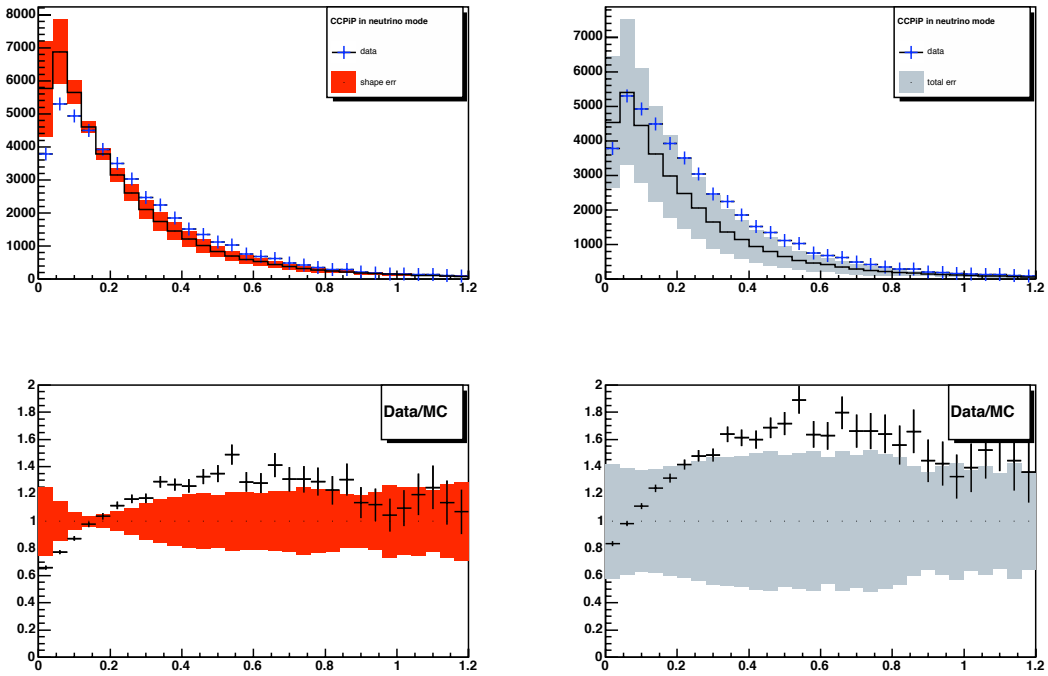

Figure 1: reconstructed Q^2 distribution and ratio for $CC\pi^+$ sample for the neutrino mode.

has one free parameter. In Nuance used in MiniBooNE prediction as default we use following values: $M_A = 1.1\ GeV$ for axial-vector form factor and $M_V = 0.84\ GeV$ for vector form factor.

The detail description of the $CC\pi^+$ samples in the neutrino and anti-neutrino modes is given in [TN244]. The $CC\pi^+$ events are produced in following reactions

- Resonant production

$$\nu + p \rightarrow \mu^- + p + \pi^+ - channel\ 3$$
$$\nu + n \rightarrow \mu^- + n + \pi^+ - channel\ 5$$

  - For the MiniBooNE beam with avarage energy about 0.7 GeV the biggest contribution comes from excitation of the $\Delta(1234)$ resonance. From the isospin consideration we know that for processes

$$\nu + p \overset{\Delta^{++}}{\Rightarrow} \mu^- + p + \pi^+$$
$$\nu + n \overset{\Delta^{+}}{\Rightarrow} \mu^- + n + \pi^+$$

relation between cross sections is following

$$\sigma(\nu + p \to \Delta^{++} + \mu^-) = 9\sigma(\nu + n \to \Delta^{+} + \mu^-) \quad (1)$$

– In channel 5 there is additional contribution from amplitudes for 1/2 isospin final state and nonresonant contribution and nuclear effects play a role. Neutrinos interact with component of CH_2, so 6 neutrons and 8 protons. The ratio of these two channels predicted by Monte Calro is about 6 (see table 1).

- Coherent production and diffractive processes are part of channel 97

  In Nuance we use for the $CC\pi^+$ coherent production 0.651 of the $NC\pi^0$ coherent production.

Table 1: The composition of the $CC\pi^+$ sample. The contribution from three $CC\pi^+$ channel are shown. The background is also shown. (may2007_2_cocktail_new)

	#events	fraction of $CC\pi^+$ sample
all $CC\pi^+$ events	168710	1
$\nu p \to \mu^- p\pi^+$ (free proton)	40719	0.24
$\nu p \to \mu^- p\pi^+$ (bound proton)	79317	0.47
$\nu n \to \mu^- n\pi^+$ (bound neutron)	20464	0.12
coherent	10229	0.061
background	22197	0.13

In table 1 prediction of $CC\pi^+$ events is shown for different channels and scattering off proton is additionally splitted into two parts, scattering off free proton and bound proton. In figure 2 the distribution of Q^2 for the $CC\pi^+$ sample is shown. The contribution form $CC\pi^+$ events from scattering on protons and bound nucleons as well as the coherent production and the background is shown. The top plot shows the absolute contributions from signal and background channels and the in bottom plot shape of distributions is compared. The coherent production is also normalized, but low Q^2 is not shown intentionally.

$CC\pi^+$ box

The $CC\pi^+$ events are those which pass following cuts [tn157]

- 3 subevents only

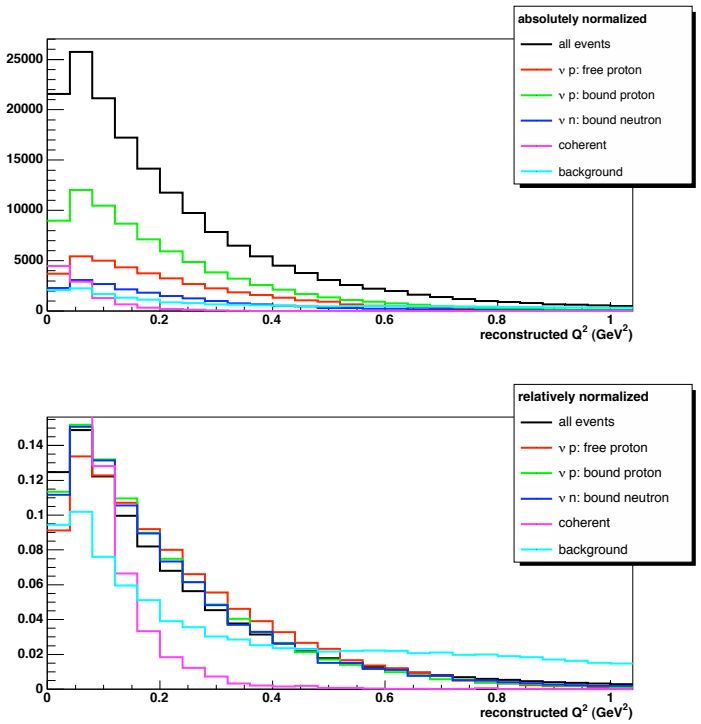

Figure 2: Distributions of the reconstructed Q^2 for various channels. The top plot shows the absolute contributions from signal channels and background and the in bottom plot shape of distributions is compared. The coherent low Q^2 is not shown intentionally.

- First subevent in the beam window and at least 175 tank hits
- All subevents have less than six veto hits
- Two subevents pass the Michel cut: 20 < tank hits < 200
- Distance between muon endpiont and nearest Michel not greater than 150 cm
- Vertex position and Michel positions are in the tank $R < 500cm$

$CC\pi^+$ box composition

The purity of the $CC\pi^+$ sample in the neutrino mode is at the level of 87% and the biggest background is the $CCQE$ reaction which accounts for about 5.2% of the sample. It is worth to notice that about 3.6% of CCQE background are event with additional pion produced in the nuclear reactions and therefore is an irreducible background. The rest of the background consists of various charged-current processes and only less than 0.5% are neutral-current reactions. In table 2 contributions to

signal and background from exclusive reactions are listed.

Table 2: $CC\pi^+$ box composition. The signal part together with the main background channel are listed.

nuance channel	reaction	contribution (%) [1]
3	$\nu_\mu p \to \mu^- p\pi^+$	**68.88**
5	$\nu_\mu n \to \mu^- n\pi^+$	**11.98**
97	$\nu_\mu A \to \mu^- \pi^+ A$	**5.87**
1	$\nu_\mu n \to \mu^- p$	5.23
4	$\nu_\mu n \to \mu^- p\pi^0$	1.48
21	$\nu_\mu n \to \mu^- \Delta^{++}\pi^-$	1.18
18	$\nu_\mu p \to \mu^- \Delta^{++}\pi^0$	1.02
91	$\nu_\mu N(= n, p) \to \mu^- X$	0.76
17	$\nu_\mu p \to \mu^- \Delta^{++}\pi^+$	0.58
67	$\nu n \to \mu^- p\eta$	0.40
20	$\nu n \to \mu^- \Delta^0\pi^+$	0.38
79	$\nu n \to \mu^- p\pi^+\pi^-$	0.31
92	$\nu_\mu N(= n, p) \to \nu_\mu X$	0.21
rest		1.82
signal	channels 3, 5 and 97	86.73

I.1 Rein-Sehgal model

This section is a compilaction of several papers cited in the text. The resonance excitation model describes 6 charged current reactions and 8 neutral current reactions.

Charged Current

$$\nu p \rightarrow \mu^- p\pi^+ \text{ (channel 3)} \qquad \bar{\nu}n \rightarrow \mu^+ n\pi^- \text{ (channel 10)} \tag{2}$$

$$\nu n \rightarrow \mu^- n\pi^+ \text{ (channel 5)} \qquad \bar{\nu}p \rightarrow \mu^+ n\pi^0 \text{ (channel 11)} \tag{3}$$

$$\nu n \rightarrow \mu^- n\pi^0 \text{ (channel 4)} \qquad \bar{\nu}p \rightarrow \mu^+ p\pi^0 \text{ (channel 12)} \tag{4}$$

Neutral Current

$$\nu p \rightarrow \nu p\pi^0 \text{ (channel 6)} \qquad \bar{\nu}p \rightarrow \bar{\nu}p\pi^0 \text{ (channel 13)} \tag{5}$$

$$\nu p \rightarrow \nu n\pi^+ \text{ (channel 7)} \qquad \bar{\nu}p \rightarrow \bar{\nu}n\pi^+ \text{ (channel 14)} \tag{6}$$

$$\nu n \rightarrow \nu n\pi^0 \text{ (channel 8)} \qquad \bar{\nu}n \rightarrow \bar{\nu}n\pi^0 \text{ (channel 15)} \tag{7}$$

$$\nu n \rightarrow \nu p\pi^- \text{ (channel 9)} \qquad \bar{\nu}n \rightarrow \bar{\nu}p\pi^- \text{ (channel 16)} \tag{8}$$

It is worth to remember that single pion can be produced without resonance excitation (nonresonant background)

Although for MiniBooNE beam pions are mainly produced due to the excitation of $\Delta(1232)$ resonance, there is non negligible contribution from resonance with isospin 1/2 such as $N(1440)$ and $N(1535)$.

From the Clebsh-Gordan coefficients one can see that amplitudes for the single pion production have a form [2]:

$$A\left(\mu^- + p + \pi^+\right) = A_3^{CC} \tag{9}$$

$$A\left(\mu^- + n + \pi^+\right) = 1/3A_3^{CC} + 2\sqrt{2}/3A_1^{CC} \tag{10}$$

$$A\left(\mu^- + p + \pi^0\right) = -\sqrt{2}/3A_3^{CC} + 2/3A_1^{CC} \tag{11}$$

$$A\left(\nu_\mu + p + \pi^0\right) = \sqrt{2}/3A_3^{NC} + 1/3A_1^{NC} + 1/3A_1^0 \tag{12}$$

$$A\left(\nu_\mu + n + \pi^+\right) = -1/3A_3^{NC} + \sqrt{2}/3A_1^{NC} + \sqrt{2}/3A_1^0 \tag{13}$$

$$A\left(\nu_\mu + n + \pi^0\right) = \sqrt{2}/3A_3^{NC} + 1/3A_1^{NC} - 1/3A_1^0 \tag{14}$$

$$A\left(\nu_\mu + p + \pi^-\right) = 1/3A_3^{NC} - \sqrt{2}/3A_1^{NC} + \sqrt{2}/3A_1^0 \tag{15}$$

where $A_3^{CC,NC}$ is amplitude for the final state with isospin 3/2, and $A_1^{CC,NC}$ is a sum of amplitudes for the final state with ispspin 1/2. A_1^0 is a sum from isoscalar contributions.

Amplitudes for the neutral current A_3^{NC}, A_1^{NC}, A_1^0 can be obtain from the amplitudes for the charged current amplitudes A_3^{CC}, A_1^{CC} by re-scaling vector and axial-vector form factors. In the case of A_3^{NC}, A_1^{NC} the vector and axial form factors need to be multiply by $1 - 2\sin^2\theta_W$ and 1, respectively. For A_1^0 we multiply form factor by $-2/3\sin\theta_W$ and 0.

The matrix element for a resonance excitation process has a following form [13]

$$T(\nu + N \to \mu^- N^*) = \frac{G_F \cos\theta_C}{\sqrt{2}}[\bar{u}_l\gamma^\beta(1-\gamma_5)u_\nu] < N^*|J_\beta^+(0)|N > \tag{16}$$

The hadronic current operator is rewritten in such a form that resonance mass M is factored out

$$J_\beta^+ = V_\beta - A_\beta = 2MF_\beta = 2M(F_\beta^V - F_\beta^A), \tag{17}$$

The lepton current is expanded in the resonance rest frame (RRF)

$$\bar{u}_l\gamma^\mu(1-\gamma_5)u_\nu|_{RRF} = -2\sqrt{2}E_\nu\sqrt{\frac{Q^2}{|\mathbf{q}|^2}}\left(ue_L^\mu - ve_R^\mu + \sqrt{2uv}e_S^\mu\right) \tag{18}$$

The vectors e_L^μ, e_R^μ and e_S^μ are polarization vectors of the virtual intermediate boson, corresponding to left-handed, right-handed, and scalar polarization

$$e_L^\mu = \frac{1}{\sqrt{2}}(0,1,-i,0) \tag{19}$$

$$e_R^\mu = \frac{1}{\sqrt{2}}(0,-1,-i,0) \tag{20}$$

$$e_S^\mu = \frac{1}{\sqrt{Q^2}}(Q^*,0,0,\nu^*) \tag{21}$$

$$e_0^\mu = (1,0,0,0) \tag{22}$$

In the resonance rest frame the matrix element takes a form

$$T(\nu + N \to \mu^- N^*) = 4G_F\cos\theta_C M_N E_\nu\left[\sqrt{\frac{Q^2}{|\mathbf{q}|^2}} < N^*|uF_- - vF_+|N > + \frac{M_N}{M}\sqrt{2uv} < N^*|F_0|N >\right] \tag{23}$$

where

$$F_+ = e_R^\mu F_\mu = -\frac{1}{\sqrt{2}}(F_x + iF_y) \tag{24}$$

$$F_- = e_R^\mu F_\mu = \frac{1}{\sqrt{2}}(F_x - iF_y) \tag{25}$$

$$F_0 = \sqrt{\frac{Q^2}{Q^{*2}}}e_S^\mu F_\mu = F_t + \frac{\nu^*}{Q}F_z \tag{26}$$

The cross section is expressed in terms of partial cross section σ_L, σ_R and σ_S instead of the ordinary structure functions W_1, W_2 and W_3

$$\frac{d\sigma}{dQ^2dW^2} = \frac{G_F^2\cos^2\theta_C}{8\pi^2 M_N}\kappa\frac{Q^2}{|\mathbf{q}|^2}\left[u^2\sigma_L + v^2\sigma_R + 2uv\sigma_S\right] \tag{27}$$

where

$$u = \frac{E_\nu + E_l + |\mathbf{q}|}{2E_\nu} \tag{28}$$

$$v = \frac{E_\nu + E_l - |\mathbf{q}|}{2E_\nu} \tag{29}$$

and κ is a flux factor

$$\kappa = \frac{W^2 - M_N^2}{2M_N} \tag{30}$$

Partial cross section σ_L, σ_R and σ_S have following forms

$$\sigma_{L,R} = \frac{\pi M}{2M_N}\frac{1}{\kappa}\sum_{j_z}|< N, j_z \mp 1|F_\mp|N^*, j_z >|^2\,\delta(W - M) \tag{31}$$

$$\sigma_S = \frac{\pi M}{2M_N}\frac{1}{\kappa}\frac{|\mathbf{q}|^2}{Q^2}\sum_{j_z}|< N, j_z|F_0|N^*, j_z >|^2\,\delta(W - M) \tag{32}$$

The $\sigma_{L,R}$ and σ_S are define in terms of the helicity amplitudes

$$f_{\pm|2j_z|} = < N, j_z \pm 1|F_\pm|N^*, j_z > \tag{33}$$

$$f_{0\pm} = \left\langle N, \pm\frac{1}{2}\,|F_0|\,N^*, \pm\frac{1}{2}\right\rangle \tag{34}$$

The helicity amplitudes are listed in the Table II of [8] and they are combinations of so called reduced matrix elements or dynamical form factors

$$T^V = \frac{1}{3W}\sqrt{\frac{\Omega}{2}}G^V(Q^2) \tag{35}$$

$$R^V = \sqrt{2}\frac{M_N}{W}\frac{(W + M_N)|\mathbf{q}|}{(W + M_N)^2 + Q^2}G^V(Q^2) = R \tag{36}$$

$$S = \frac{Q^2}{|\mathbf{q}|^2}\frac{3WM_N - Q^2 - M_N^2}{6M_N^2}G^V(Q^2) \tag{37}$$

$$T^A = \frac{2}{3}\sqrt{\frac{\Omega}{2}}\frac{M_N}{W}\frac{|\mathbf{q}|}{(W + M_N)^2 + Q^2}ZG^A(Q^2) \tag{38}$$

$$R^A = \frac{\sqrt{2}}{6W}\left(W + M_N + \frac{2n\Omega W}{(W + M_N)^2 + Q^2}\right)ZG^A(Q^2) \tag{39}$$

$$B = \frac{1}{3W}\sqrt{\frac{\Omega}{2}}\left(1 + \frac{W^2 - M_N^2 - Q^2}{(W + M_N)^2 + Q^2}\right)ZG^A(Q^2) \tag{40}$$

$$C = \frac{1}{6M_N|\mathbf{q}|}\left(W^2 - M_N^2 + n\Omega\frac{W^2 - M_N^2 - Q^2}{(W + M_N)^2 + Q^2}\right)ZG^A(Q^2) \tag{41}$$

where $\Omega = 1.05GeV^2$ was determined form the Regge slope of baryon trajectory, N is a number of the oscillator quanta in the final state and Z is a renormalization factor. The renormalization constant Z compensate the difference between the value of the axial vector form factor for $Q^2 = 0$ predicted by the FKR model 5/4 and experimental value. In the paper by Rein and Sehgal the experimental value was $1.25 = 4/3$ therefore and $Z = 3/4$. The value $Z = 0.76$ used in Nuance was determined by Gerry Garvey who took the newest value of $g_A = 1.2671$.

The axial-vector form factor has a form :

$$\bar{G}_A^{RS} = \frac{Z g_A}{\left(1 + \frac{Q^2}{M_A^2}\right)^2}. \tag{42}$$

The vector form factor has a form

$$G_V^{RS} = \frac{1}{\left(1 + \frac{Q^2}{M_V^2}\right)^2} \tag{43}$$

The vector and axial vector form factor are modified by a resonant number dependent factor

$$G_{res}^{corr} = \left(1 + \frac{Q^2}{4M^2}\right)^{\frac{1}{2}-N} \tag{44}$$

The correction factor can have different form, which will be discussed in following sections.

II Modifications of the Rein-Sehgal model

The hadronic current for the resonance excitation consists both vector and axial vector form factors. For the Δ resonance, which is a Rarita-Schwinger spinor use use following parametrization of the hadronic curren

$$< \Delta^{++}|J^\nu|p >= \sqrt{3}\bar{\psi}_\lambda(P) d^{\lambda\nu} u(p), \tag{45}$$

where ψ_λ is a Rarita-Schwinger spinor, $u(p)$ is a Dirac spinor and $d^{\lambda\nu}$ has following form

$$\begin{aligned} d^{\lambda\nu} &= g^{\lambda\nu}\left[\frac{C_3^V}{M}\not{q} + \frac{C_4^V}{M^2}(Pq) + \frac{C_5^V}{M^2}(pq) + C_6^V\right]\gamma_5 - q^\lambda\left[\frac{C_3^V}{M}\gamma^\nu + \frac{C_4^V}{M^2}P^\nu + \frac{C_5^V}{M^2}p^\nu\right]\gamma_5 \\ &+ g^{\lambda\nu}\left[\frac{C_3^A}{M}\not{q} + \frac{C_4^A}{M^2}(Pq)\right] - q^\lambda\left[\frac{C_3^A}{M}\gamma^\nu + \frac{C_4^A}{M^2}P^\nu\right] + g^{\lambda\nu}C_5^A + q^\lambda q^\nu\frac{C_6^A}{M^2} \end{aligned} \tag{46}$$

The conserved vector current (CVC) hypothesis requires $C_6^V = 0$. From the partially conserved axial current hypothesis we know the form factor C_6^A is connected to the C_5^A

$$C_6^A = C_5^A \frac{M^2}{m_\pi^2 - q^2}. \tag{47}$$

With a couple of assumptions one can find a relationships between helicity amplitudes and current in the Rarita-Schwinger formalism [6].

II.1 Axial-vector form factor in the Rein-Sehgal model

The relationship between the axial-vector form factor in the Rein-Sehgal model and in the Rarita-Schwinger model has been obtained by Graczyk and Sobczyk [6]. They assumed the Adler's relation

$$C_4^A = -\frac{1}{4}C_5^A \tag{48}$$

$$C_3^A = 0 \tag{49}$$

Then G_A and C_5^A are related

$$\bar{G}_A^{new} = \frac{\sqrt{3}}{2}\left(1+\frac{Q^2}{(M+W)^2}\right)^{\frac{1}{2}-N}\left[1-\frac{W^2-Q^2-M^2}{8M^2}\right]C_5^A \tag{50}$$

There are two versions of C_5^A proposed by Lalakulich et a., [10] to fit to BNL and ANL data separately

$$C_5^{A,ANL} = C_5^A(0)\left(1+\frac{Q^2}{M_A^2}\right)^{-2}\left(1+2\frac{Q^2}{M_A^2}\right)^{-1}, \tag{51}$$

$$C_5^{A,BNL} = C_5^A(0)\left(1+\frac{Q^2}{M_A^2}\right)^{-2}\left(1+\frac{Q^2}{3M_A^2}\right)^{-1} \tag{52}$$

where

$$C_5^A(0) = \frac{g_{\Delta N\pi}f_\pi}{\sqrt{6}M} \approx 1.2 \tag{53}$$

From lattice QCD calculation it is justified to set the $C_5^A(0)$ to about 0.8, and Hernandez et al. [12] found that for the ANL data the best values of $C_5^A(0)$ is 0.867 ± 0.075 with axial mass $M_A = 0.985$.

In figure 3 the shape of the axial-vector form factor as a function of Q^2 for different values of the axial mass and the its ratio and the one for $M_A = 1.1GeV$ is shown. The Nuance predictions for the generated and reconstructed Q^2 is presented in figure 4. For higher values of the axial mass the cross section for the low Q^2 is suppressed. Although the higher values of axial mass give a suppression of the cross section for low Q^2, the shape and the high Q^2 tail behavior suggest that it may be just a part of the solution.

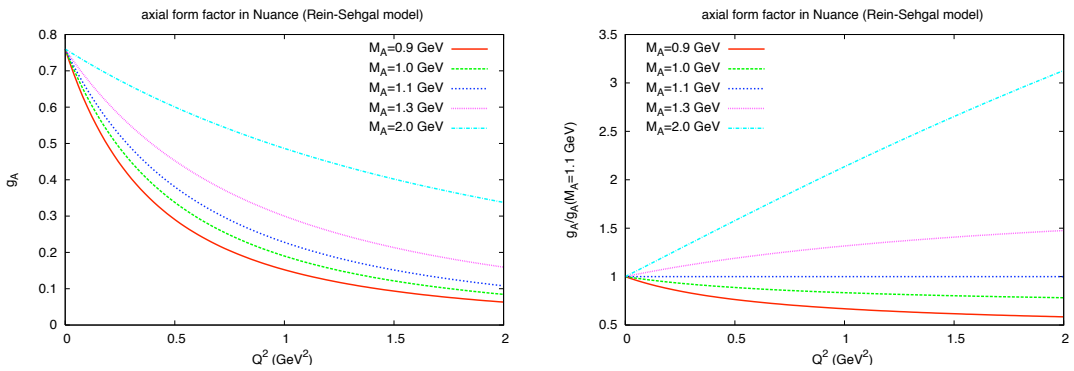

Figure 3: The axial-vector form factor for the Rein-Sehgal model for various values of axial mass (left). The ratio of prediction for new value of M_A and prediction for $M_A = 1.1\ GeV$ is shown on the right.

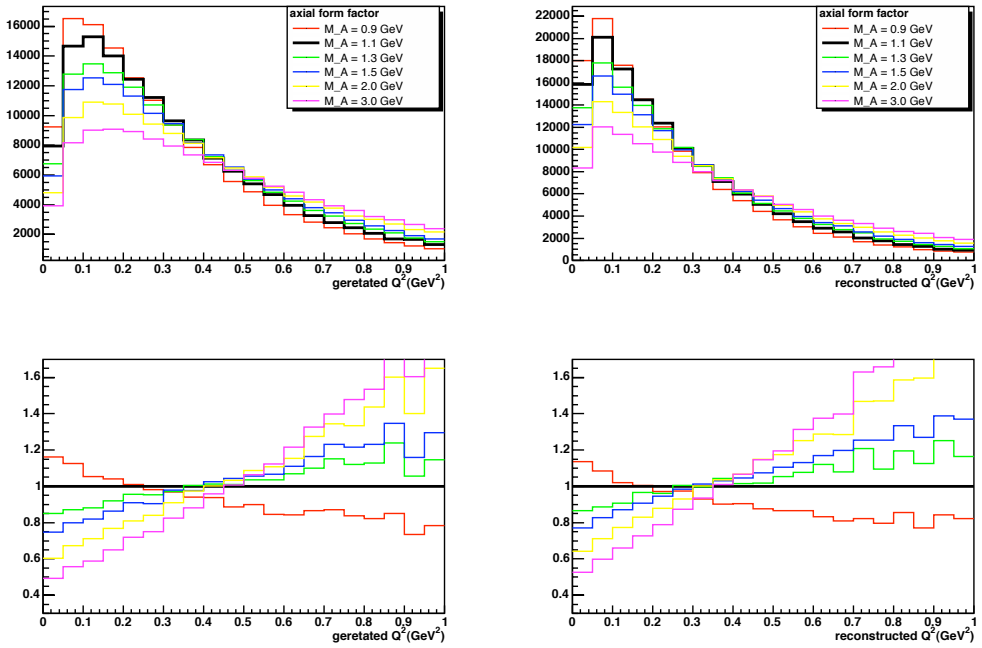

Figure 4: Nuance predictions for various axial-vector mass value in the Rein-Sehgal model.

II.2 Form factors correction

The vector and axial-vector form factors in the RS model can be factorized into two parts, the dipol form and the dependent on the resonance number. It is assumed the the resonance dependent part has the same form for both form factors.

$$G_V^{RS} = \left(1 + \frac{Q^2}{M_V^2}\right)^{-2} G_{res} \tag{54}$$

$$G_A^{RS} = 0.76 \left(1 + \frac{Q^2}{M_A^2}\right)^{-2} G_{res} \tag{55}$$

The form of this correction might be chosen from several possibilities. In the Rein and Sehgal paper [8] two forms are presented, but in the Nuance the third one is used.

electron-type: the form used in the case of electron scattering [4]

$$G_{res}^{e-type} = \left(1 + \frac{Q^2}{4W^2}\right)^{\frac{1}{2}(1-N)} \tag{56}$$

neutrino-type: the form proposed for the neutrino scattering [5]

$$G_{res}^{nu-type} = \left(1 + \frac{Q^2}{4M_{nucleon}^2}\right)^{\frac{1}{2}-N} \tag{57}$$

Nuance The resonance correction for the form factors implemented in Nuance [9] has the same form as the one for the electron scattering but with nucleon mass instead of resonance mass [2]

$$G_{res}^{Nuance} = \left(1 + \frac{Q^2}{4M_{nucleon}^2}\right)^{\frac{1}{2}(1-N)} \tag{58}$$

In figure 5 form factor corrections are shown and their effect on the dipole form of vector and axial vector form factors. Alghough the corrections look as a significant one they only slightly modify form factor (biggest change for N=2) . In figure 6 the comparision of the three versions of the correction due to resonance number in the Nuance predictions is shown and its modification of the form factors. The changes introduced by different form of form factor corrections is virtual and negligible.

[2] Rein and Seghal cite the Ravndal paper [14] as a source of the form with nucleon mass but in pointed equation M denote resonance mass.

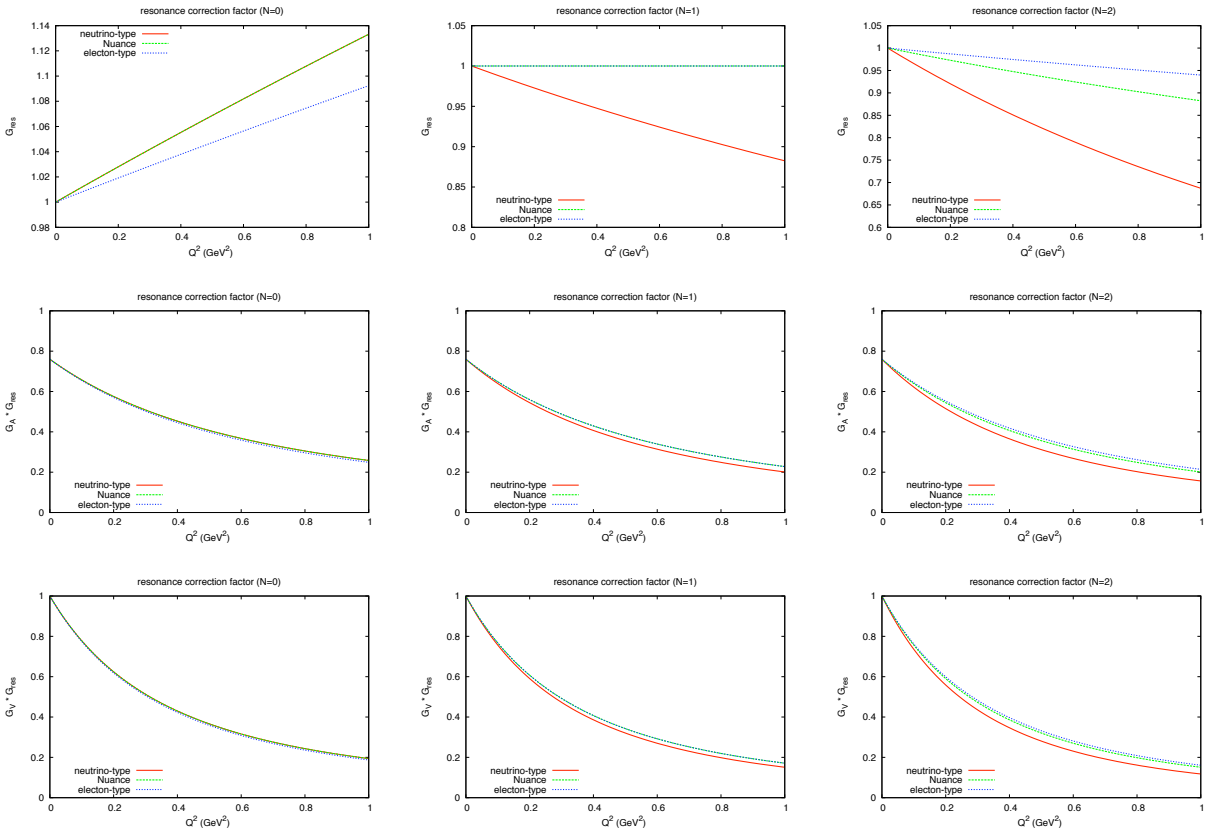

Figure 5: The resonance correction of form factors in the Rein-Sehgal model. In top row the corrections is shown alone while in middle and bottom rows its affect on the axial and vector form factors is presented. Each column represent the given oscillator quanta.

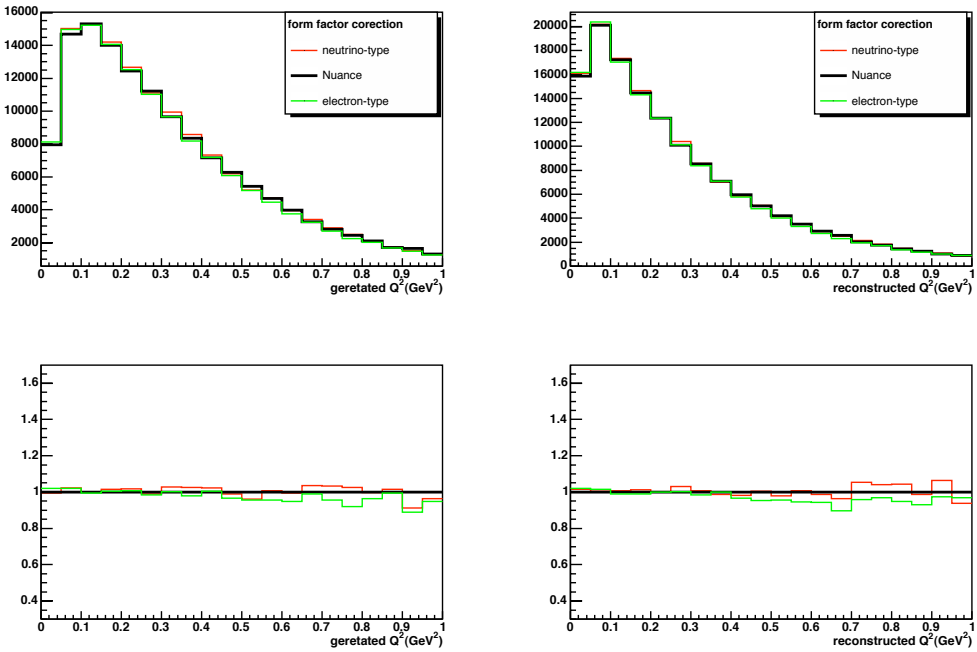

Figure 6: Nuance predictions for three versions of the correction. The difference between form factor corrections are negligible.

II.3 Fitting Rein-Sehgal to the ANL and BNL data

The relation between the axial-vector form factor G_A and the form factor C_5^A is following

$$\bar{G}_A^{new} = \frac{\sqrt{3}}{2}\left(1+\frac{Q^2}{(M+W)^2}\right)^{\frac{1}{2}}\left(1+\frac{Q^2}{4M^2}\right)^{-N}\left[1-\frac{W^2-Q^2-M^2}{8M^2}\right]C_5^A \tag{59}$$

The available data from ANL [21] and BNL [22] experiments are expressed in the term of the C_5^A. Measured $CC\pi^+$ sample for ANL and BNL were obtained from the neutrino interaction with deuterium target. Having the relation 59 we can fit parameters from the RS model to the data. In the RS the axial-vector has a form

$$\bar{G}_A^{RS} = 0.76\left(1+\frac{Q^2}{M_A^2}\right)^{-2}\left(1+\frac{Q^2}{4M^2}\right)^{\frac{1}{2}-N} \tag{60}$$

We rewrote the formula in such a form that we can fit two parameters M_A and $G_A^{RS}(0)$. The axial-vector form factor has a form

$$C_5^A = \frac{\bar{G}_A^{RS}(0)\left(1+\frac{Q^2}{M_A^2}\right)^{-2}\left(1+\frac{Q^2}{4M^2}\right)^{\frac{1}{2}}}{\frac{\sqrt{3}}{2}\left(1+\frac{Q^2}{(M+W)^2}\right)^{-\frac{1}{2}}\left[1-\frac{W^2-Q^2-M^2}{8M^2}\right]^{-1}} \tag{61}$$

In the first step we set only one free parameter M_A and fit it to three samples of data with following results

ANL sample only

$$M_A = 0.912GeV \tag{62}$$

BNL sample only

$$M_A = 0.972GeV \tag{63}$$

ANL and BNL samples

$$M_A = 0.956GeV \tag{64}$$

In figure 7 the ANL and BNL data results for the C_5^A and fitted axial form factor from the Rein-Sehgal model is shown. The shape of the form factor and values of M_A in all three cases are very similar and we do not expect significant difference in the simulation performed by Nuance.

Since the fitting to the RS model gave change in the direction like observed for the lower then default value of the axial mass changes we decided to introduce a second free parameter. In addition to the M_A the secod free parameter will be a value of the axial-vector form factor in the limit $G_A^{RS}(Q^2 \to 0)$. Fitted values of RS parameters for the axial-vector form factor are

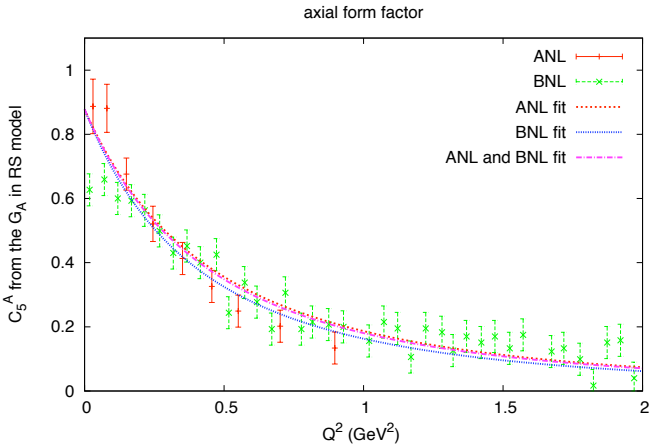

Figure 7: The ANL and BNL data for the axial-vector form factor C_5^A with the fitted curves to the form obtained form the Rein-Sehgal model with one free parameter M_A.

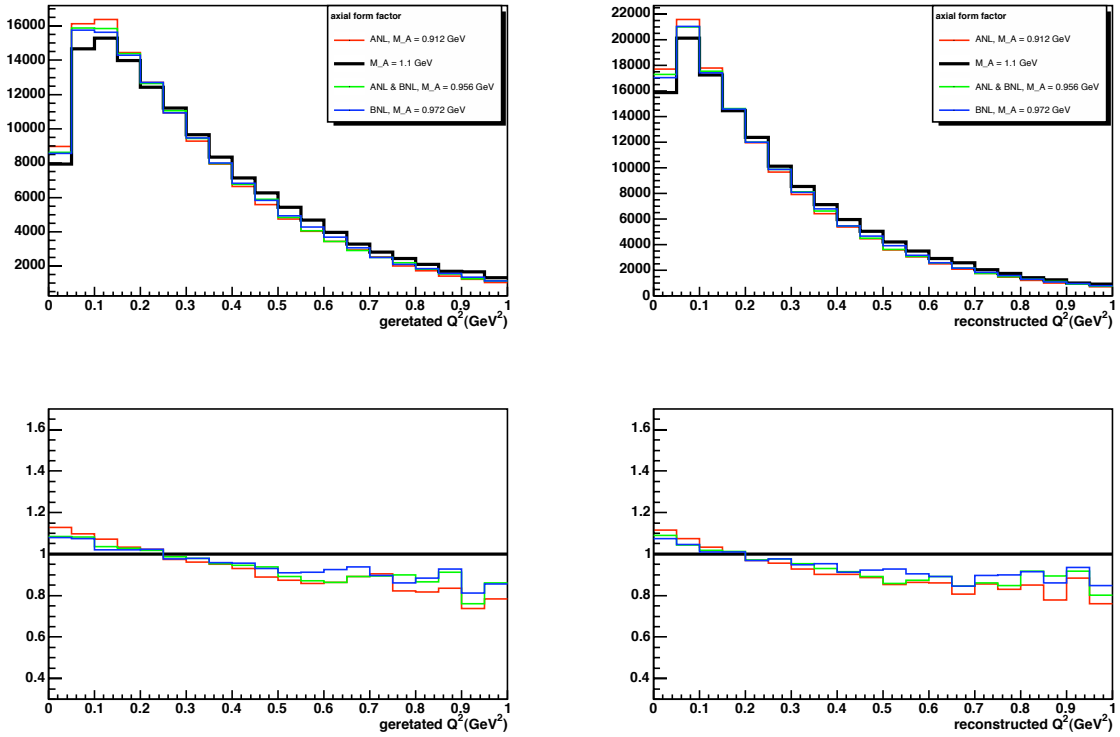

Figure 8: Nuance predictions for three set of M_A and $G_A^{RS}(0)$ values obtained form fitting to ANL and BNL data.

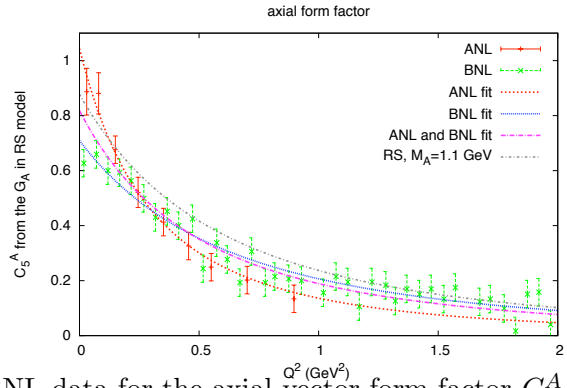

Figure 9: The ANL and BNL data for the axial-vector form factor C_5^A with the fitted curves to the form obtained form the Rein-Sehgal model.

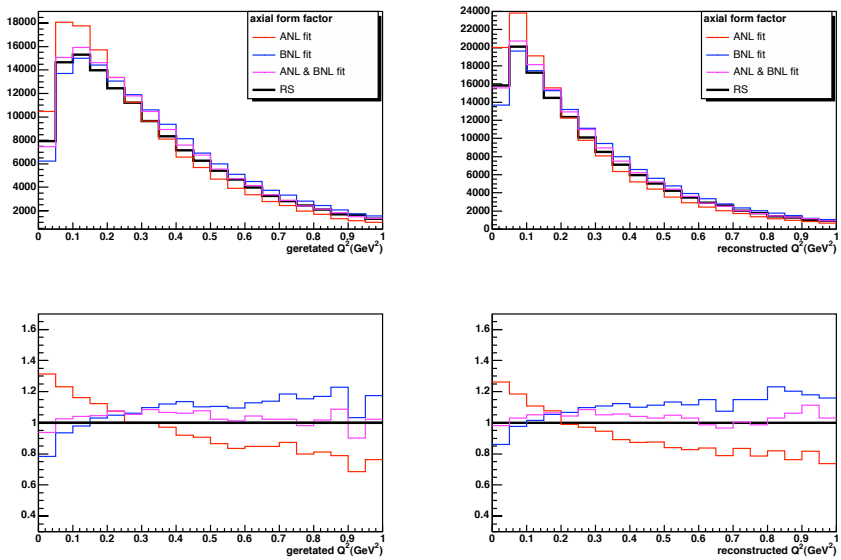

Figure 10: Nuance predictions for three set of M_A and $G_A^{RS}(0)$ values obtained form fitting to ANL and BNL data.

ANL sample only

$$M_A = 0.783 GeV \text{ and } G_A^{RS}(0) = 0.903 \tag{65}$$

BNL sample only

$$M_A = 1.148 GeV \text{ and } G_A^{RS}(0) = 0.614 \tag{66}$$

ANL and BNL samples

$$M_A = 1.013 GeV \text{ and } G_A^{RS}(0) = 0.708 \tag{67}$$

Figure 9 shows a fitted form factor for three cases. This time the values for $Q^2 \to 0$ vary form case to case, and the shape is different. In figure 10 the results from the Nuance are shown. The fit

to the ANL data gives the worst prediction of the resonance production of the $CC\pi^+$ events.

II.4 Fits of new axial vector form factor

At least three groups tried to fit the existing data to the axial vector form factor in the Rarita-Schwinger formalism. Using the formula (59) from [6] we applied them Rein-Sehgal model. Following forms of the C_5^A were used

Hernandez et al. $C_5^A(0) = 0.867$, $M_A = 0.985GeV$**:**

$$C_5^A = C_5^A(0)\left(1 + \frac{Q^2}{M_A^2}\right)^{-2}\left(1 + \frac{Q^2}{3M_A^2}\right)^{-1} \tag{68}$$

Graczyk and Sobczyk v1 $C_5^A(0) = 1.2$, $m_a = 0.54GeV^2$**:**

$$C_5^A = C_5^A(0)\left(1 + \frac{Q^2}{m_a}\right)^{-2} \tag{69}$$

Graczyk and Sobczyk v2 $C_5^A(0) = 0.88$, $m_a = 9,71GeV^2$, $m_b = 0.35GeV^2$**:**

$$C_5^A = C_5^A(0)\left(1 + \frac{Q^2}{m_a}\right)^{-2}\left(1 + \frac{Q^2}{m_b}\right)^{-1} \tag{70}$$

Lalkulich et al. v1, $C_5^A(0) = 1.2$, $M_A = 1.1GeV$**:**

$$C_5^A = C_5^A(0)\left(1 + \frac{Q^2}{M_A^2}\right)^{-2}\left(1 + 2\frac{Q^2}{M_A^2}\right)^{-1} \tag{71}$$

Lalakulich et al., v2 $C_5^A(0) = 1.2$, $M_A = 1.1GeV$**:**

$$C_5^A = C_5^A(0)\left(1 + \frac{Q^2}{M_A^2}\right)^{-2}\left(1 + \frac{Q^2}{3M_A^2}\right)^{-1} \tag{72}$$

From lattice QCD calculation it is justified to set it to about 0.8, and Hernandez et al. fitted it to the ANL data to be 0.867

In the limit $Q^2 \to 0$ the eq. (59) gives following relation

$$G_A(0) = \frac{\sqrt{3}}{2}\left(1 - \frac{W^2 - M^2}{8M^2}\right)C_5^A(0) \tag{73}$$

which with $W = 1.234\ GeV$ gives us a value

$$C_5^A(0) = 0.97 \tag{74}$$

In figure 11 various forms of the axial vector form factors are shown as a function of Q^2. The Rein-Sehgal parametrization was obtained by applying eq. (59) to the dipole form. In figures 12 and 13 the modifications in predicted number of events for different parametrization of the C_5^A if presented.

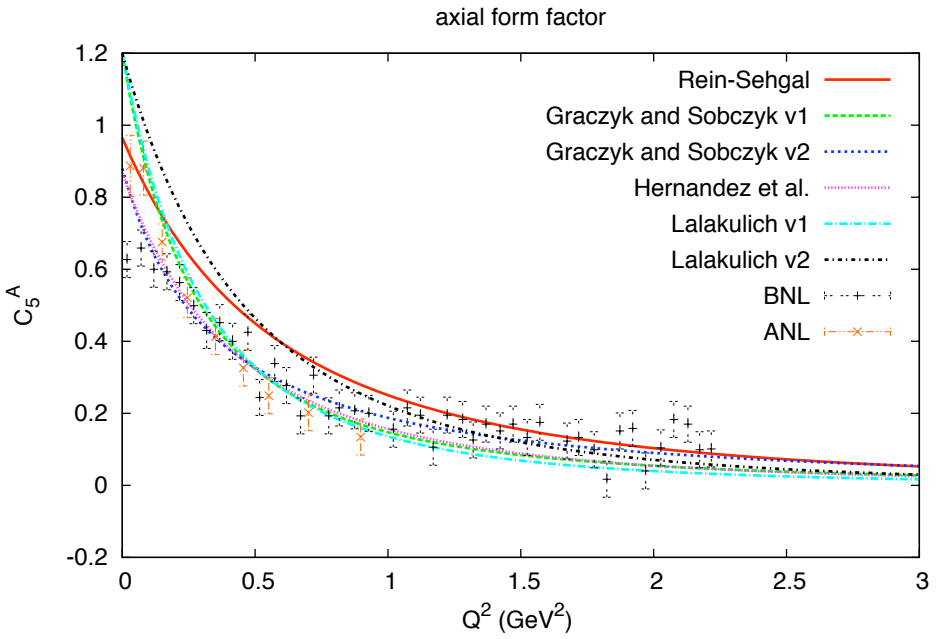

Figure 11: The axial vector form factor C_5^A for different parametrizations.

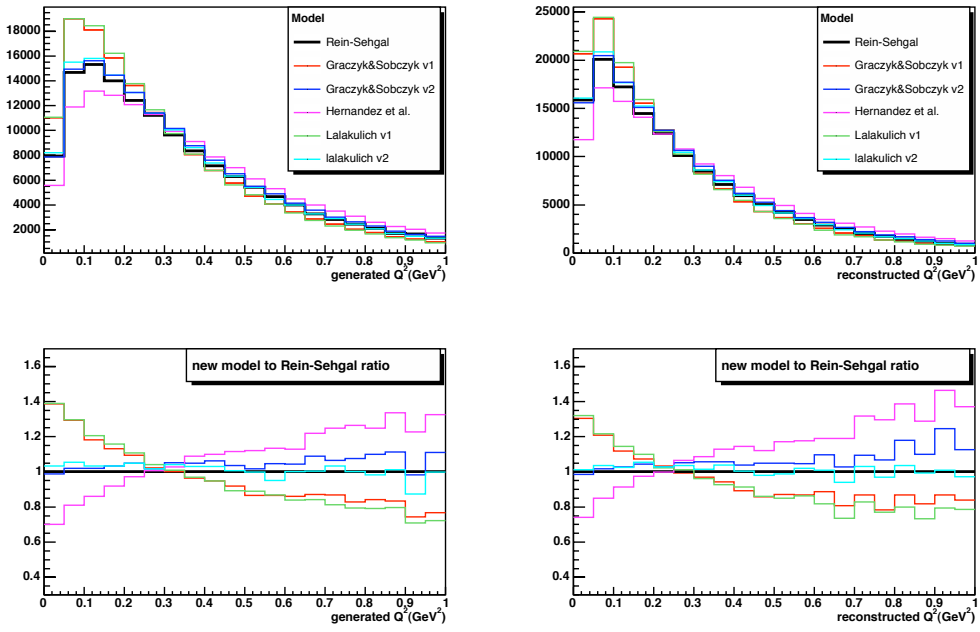

Figure 12: Nuance predictions for $Q2$ distribution of $CC\pi^+$ events for 5 forms of axial vector form factor available in literature.

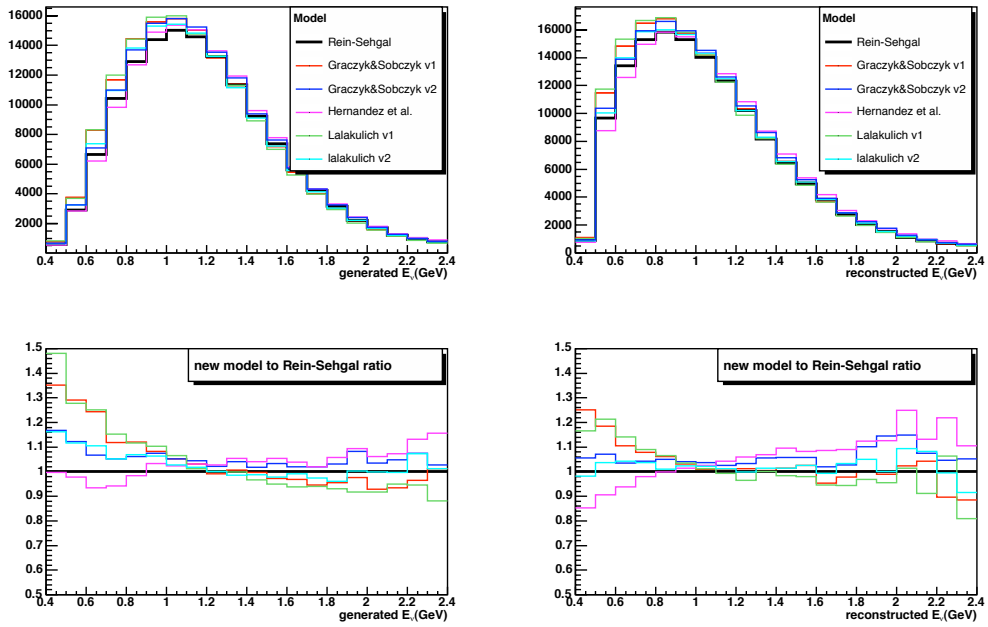

Figure 13: Nuance predictions for E_ν distribution of $CC\pi^+$ events for 5 forms of axial vector form factor available in literature.

II.5 New vector form factor

The relation between vactor form factor G_V in the RS model and form factors C_3^V, C_4^V and C_5^V is following

$$G_V^{new} = \frac{1}{2}\left(1+\frac{Q^2}{(M+W)^2}\right)^{\frac{1}{2}-N}\sqrt{3(G_3^V)^2+(G_1^V)^2} \tag{75}$$

where

$$G_3^V = \frac{1}{2\sqrt{3}}\left[C_4V\frac{W^2-Q^2-M^2}{2M^2}+C_5^V\frac{W^2+Q^2-M^2}{2M^2}+C_3^V\frac{W+M}{M}\right] \tag{76}$$

$$G_1^V = -\frac{1}{2\sqrt{3}}\left[C_4V\frac{W^2-Q^2-M^2}{2M^2}+C_5^V\frac{W^2+Q^2-M^2}{2M^2}-C_3^V\frac{M^2+Q^2+MW}{MW}\right] \tag{77}$$

And C_i^V were proposed by Lalakulich et a. [10]

$$C_3^V = 2.13\left(1+\frac{Q^2}{4M_V^2}\right)^{-1}\left(1+\frac{Q^2}{M_V^2}\right)^{-2} \tag{78}$$

$$C_4^V = -1.51\left(1+\frac{Q^2}{4M_V^2}\right)^{-1}\left(1+\frac{Q^2}{M_V^2}\right)^{-2} \tag{79}$$

$$C_5^V = 0.48\left(1+\frac{Q^2}{4M_V^2}\right)^{-1}\left(1+\frac{Q^2}{0.766M_V^2}\right)^{-2}$$

The limit for the $Q^2 \to 0$ gives following value $G_V^{new}(0) = 1.285$. It is higher the one assumed in the RS model. The difference comes from the fact that with above shown choice of form factors C_V^i it is not possible to reproduce the quark model prediction vanishing electric contribution.

In figure 14 the old and new vector for factor are shown and in figure 15 the difference in predicted ccpip production is compared for both forms of vector form factor. The new vector form factor can reduce the low Q^2 discrepancy of about 10%. In further analysis we will not include this effect, but it will be implemented in the MiniBooNE Analysis Framework.

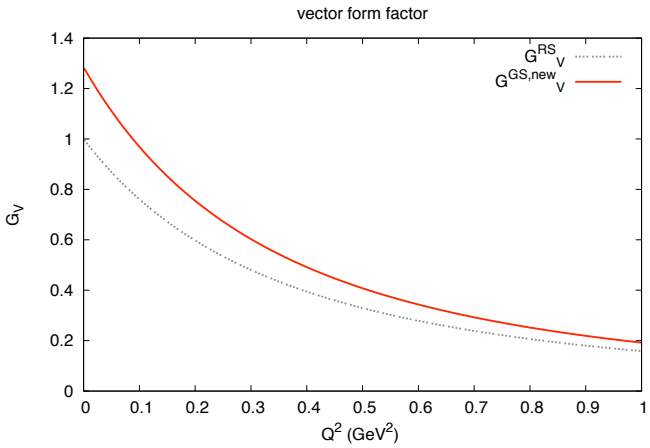

Figure 14: The vector form factor in the Rein-Sehgal model (dashed line) and the new one obtained from form factor C_i^V using eq. (75) assuming the mass of the Δ resonance.

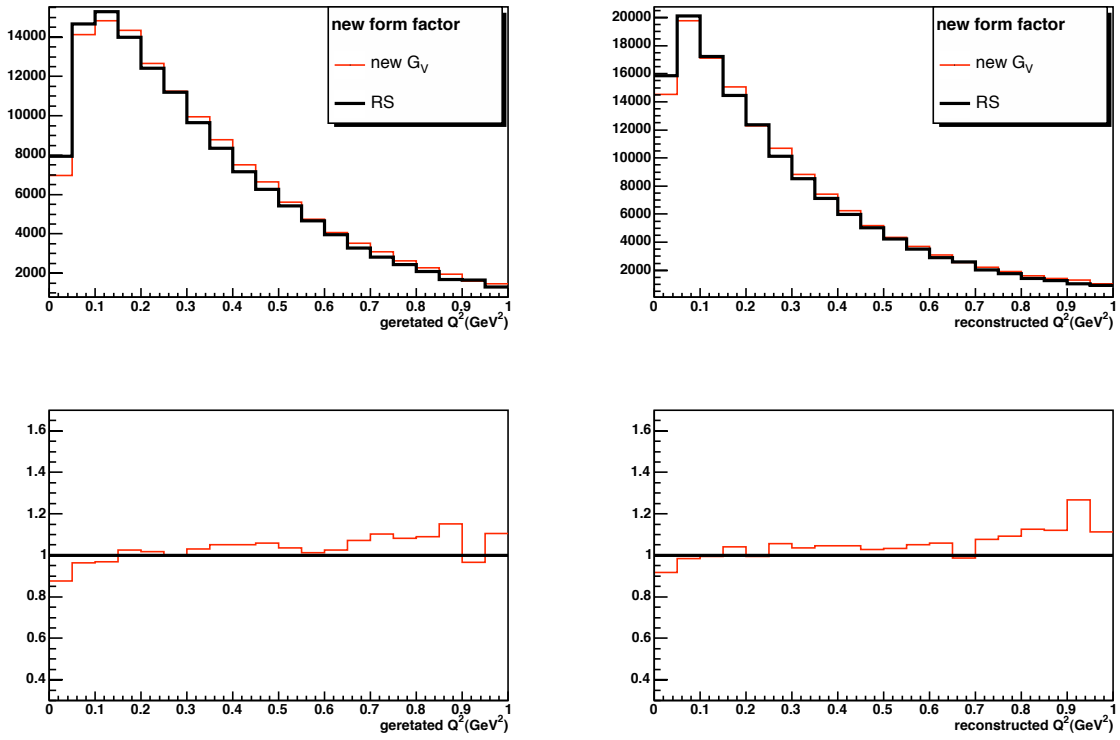

Figure 15: Nuance predictions for modified vector form factor. The effect of inclusion of new from of the vector form factors will result in a model which better represents our data.

III Muon mass effect

In RS model charged leptons are massless but there are at least three models describing how one can extend the RS model for massive leptons.

- KLN model - Kuzmin, Lyubushlin and Naumov [15]. Muon mass included only in the lepton current.
- BRS model - Berger and Sehgal [16]. Improving the KLN model by including the pion-pole contribution.
- GS model - Graczyk and Sobczyk [18]. Independent calculation with the lepton current modification and pion-pole contribution.

These modifications are not implemented in the Nuance yet.

III.1 KLN model - Kuzmin, Lyubushlin and Naumov[15]

For model with introduced final lepton mass partial cross sections depend on the helicity λ

$$\frac{d\sigma}{dQ^2dW^2} = \frac{G_F^2\cos\theta_C}{8\pi^2 M_N}\kappa\frac{Q^2}{|\mathbf{q}|^2}\sum_{\lambda=\pm}\left[\left(c_L^\lambda\right)^2\sigma_L^{(\lambda)} + \left(c_R^\lambda\right)^2\sigma_R^{(\lambda)} + \left(c_S^\lambda\right)^2\sigma_S^{(\lambda)}\right] \tag{80}$$

where in the limit of massless lepton in the final state ($m_l \to 0$), $c_L^{(-)} \to u$, $c_R^{(-)} \to v$, $c_S^{(-)} \to 2uv$ and $c_{L,R,S}^{(+)} \to 0$.

In the KLN [15] model the 4-momentum transfer in the resonance rest frame is define as $q^\mu = (\nu^*, 0, 0, Q^*)$. However, the variable $|\mathbf{q}|^*$ is also use and has the same meanig as Q^*.

In the KLN model the components of the lepton current in the RRF depend on helicity and for neutrinos can be written in the following form[3]:

$$\begin{aligned}
j^*_{0(\lambda)} &= A_\lambda\frac{1}{W}\sqrt{1-\lambda\cos\theta}\,(M_N - E_l - \lambda P_l)\\
j^*_{x(\lambda)} &= A_\lambda\frac{1}{|\mathbf{q}|}\sqrt{1+\lambda\cos\theta}\,(P_l - \lambda E_\nu)\\
j^*_{y(\lambda)} &= i\lambda A_\lambda\sqrt{1+\lambda\cos\theta}\\
j^*_{z(\lambda)} &= A_\lambda\frac{1}{|\mathbf{q}|\mathbf{W}}\sqrt{1-\lambda\cos\theta}\,[(E_\nu + \lambda P_l)(M_N - E_l) + P_l(\lambda E_\nu + 2E_\nu\cos\theta - P_l)]
\end{aligned} \tag{81}$$

[3] In the Berger and Rein paper in the component j_x is a misprint,E_l instead of E_ν

where all variables without star are quantities in the laboratory frame, and

$$A_{(\lambda)} = \sqrt{E_\nu \left(E_l - \lambda P_l\right)}. \tag{82}$$

Now the three polarization vectors have a form

$$\begin{aligned} e^\mu_L &= \frac{1}{\sqrt{2}}(0,1,-i,0) && (83)\\ e^\mu_R &= \frac{1}{\sqrt{2}}(0,-1,-i,0) && (84)\\ e^\mu_{(\lambda)} &= \frac{1}{\sqrt{Q^2}}(Q^*_{(\lambda)},0,0,\nu^*_{(\lambda)}) && (85)\\ & && (86) \end{aligned}$$

where

$$\begin{aligned} Q^*_{(\lambda)} &= \sqrt{Q^2}\frac{j_0^{*(\lambda)}}{\sqrt{\left|\left(j_0^{*(\lambda)}\right)^2 - \left(j_z^{*(\lambda)}\right)^2\right|}} && (87)\\ \nu^*_{(\lambda)} &= \sqrt{Q^2}\frac{j_z^{*(\lambda)}}{\sqrt{\left|\left(j_0^{*(\lambda)}\right)^2 - \left(j_z^{*(\lambda)}\right)^2\right|}} && (88) \end{aligned}$$

The coefficients are given by

$$\begin{aligned} c_L^{(\lambda)} &= \frac{K}{2}\left[j_x^{*(\lambda)} + i j_y^{*(\lambda)}\right] && (89)\\ c_R^{(\lambda)} &= \frac{K}{2}\left[j_x^{*(\lambda)} - i j_y^{*(\lambda)}\right] && (90)\\ c_S^{(\lambda)} &= K\sqrt{\left|\left(j_0^{*(\lambda)}\right)^2 - \left(j_z^{*(\lambda)}\right)^2\right|} && (91) \end{aligned}$$

$$K = \frac{|\mathbf{q}|}{E_\nu\sqrt{2Q^2}} \tag{92}$$

and three dynamical form factors are modified in following way

$$\begin{aligned} S \to S_{KLN} &= \left(\nu^*_{(\lambda)}\nu^* - Q^*_{(\lambda)}|\mathbf{q}^*|\right)\left(1 + \frac{Q^2}{M_N^2} - \frac{3W}{M_N}\right)\frac{G^V(Q^2)}{6|\mathbf{q}|^{\mathbf{2}}} && (93)\\ B \to B_{KLN} &= \sqrt{\frac{\Omega}{2}}\left(Q^*_{(\lambda)} + \nu^*_{(\lambda)}\frac{|\mathbf{q}^*|}{aM_N}\right)\frac{ZG^A(Q^2)}{3W|\mathbf{q}^*|} && (94)\\ C \to C_{KLN} &= \left[\left(Q^*_{(\lambda)}|\mathbf{q}^*| - \nu^*_{(\lambda)}\nu^*\right)\left(\frac{1}{3} + \frac{\nu^*}{aM_N}\right)\right.\\ &\quad \left. + \nu^*_{(\lambda)}\left(\frac{2}{3}W - \frac{Q^2}{aM_N} + \frac{n\Omega}{3aM_N}\right)\right]\frac{ZG^A(Q^2)}{2W|\mathbf{q}^*|} && (95) \end{aligned}$$

$$\nu^* = E^*_\nu - E^*_l = \frac{M_N\nu - Q^2}{W} \tag{96}$$

$$Q^* = \sqrt{Q^2 + \nu^{*2}} \tag{97}$$

$$a = 1 + \frac{W^2 + Q^2 + M_N^2}{2M_N W} \tag{98}$$

and where again Z is a renormalization factor for the axial vactor current, Ω is the slope of the baryon trajectory and N is a number of oscillator quanta in the final state [4].

The lepton current in the case of antineutrino interaction in related to the the lepton current n neutrino interaction by

$$\bar{j}^\mu_\lambda = -\lambda (j^\mu_{-\lambda})^* \tag{99}$$

which results in the following retaliations

$$[Q^*_{(\lambda)}]_{\bar{\nu}} = [Q^*_{(-\lambda)}]_\nu \tag{100}$$

$$[\nu^*_{(\lambda)}]_{\bar{\nu}} = [\nu^*_{(-\lambda)}]_\nu \tag{101}$$

and

$$[c^\lambda_L]_{\bar{\nu}} = \lambda [c^{(-\lambda)}_R]_\nu, \quad [c^\lambda_R]_{\bar{\nu}} = \lambda [c^{(-\lambda)}_L]_\nu, \quad [c^\lambda_S]_{\bar{\nu}} = -\lambda [c^{(-\lambda)}_S]_\nu \tag{102}$$

III.2 BRS model - Berger and Sehgal model

An axial hadronic current has, in addition to the quark current A_μ, a poion-pole contribution, dictated by PCAC, which modifies the axial current as follows

$$A_\mu \to \bar{A}_\mu = A_\mu + q_\mu \frac{q^\mu A_\mu}{m^2_\pi + Q^2} \tag{103}$$

In the case of massless lepton in the final state the additional term vanish when contracted with lepton current. For massive lepton, the pion-pole term doesn't vanish and the divergence of $\bar{A}_\mu$ is

$$q^\mu \bar{A}_\mu = \frac{m^2_\pi}{m^2_\pi + Q^2} q^\mu A_\mu. \tag{104}$$

This modification, as shown in [13] for axial vector current leads to matrix elements for the queasielastic process $\nu_\mu + n \to \mu^- + p$ of the form

$$< p|\bar{A}_\mu|n >= \bar{u}_p \left[\gamma_\mu\gamma_5 F^A_1(Q^2) + q_\mu\gamma_5 F^A_2(Q^2)\right] u_n \tag{105}$$

[4] in Berger and Sehgal paper $|\mathbf{q}^*|$ is used instead of Q^*

where

$$F_2^A(Q^2) = F_1^A(Q^2)\frac{2M_N + \frac{m_\pi^2}{M_N}}{m_\pi^2 + Q^2} \tag{106}$$

This result implies a induced pseudoscalar form factor

$$F_2^A(0) = \frac{2M_N}{m_\pi^2} g_A(0) \tag{107}$$

with $g_A(0) = 1.25$. Which agrees with the PCAC result

$$F_2^A(0)|_{PCAC} = \sqrt{2} g_{NN\pi} f_\pi / m_\pi^2. \tag{108}$$

Including the lepton mass and pion-pole requires modifications of two dynamical form factors w.r.t. modification done for the KLN model [16, 17]

$$S_{BRS}^{(\lambda)} = S_{KLN}^{(\lambda)} \tag{109}$$

$$B_{BRS}^{(\lambda)} = B_{KLN}^{(\lambda)} + \frac{ZG^A(Q^2)}{2WQ^*}\left(Q_{(\lambda)}^* \nu^* - \nu_{(\lambda)}^* Q^*\right)\frac{\frac{2}{3}\sqrt{\frac{\Omega}{2}}\left(\nu^* + \frac{Q^{*2}}{M_N a}\right)}{m_\pi^2 + Q^2} \tag{110}$$

$$C_{BRS}^{(\lambda)} = C_{KLN}^{(\lambda)} + \frac{ZG^A(Q^2)}{2WQ^*}\left(Q_{(\lambda)}^* \nu^* - \nu_{(\lambda)}^* Q^*\right)\frac{Q^*\left(\frac{2}{3}W - \frac{Q^2}{M_N a} + \frac{n\Omega}{3M_N a}\right)}{m_\pi^2 + Q^2} \tag{111}$$

In figure 16 the Nuance prediction for resonant production of the $CC\pi^+$ events is shown for Rein-Sehgal model and its modifications for the muon mass. In figure 17 the generated and reconstructed distribution for the $CC\pi^+$ events are shown. The modification for the new form of the axial-vector form factor is shown together with muon mass effect by BRS. In the contrast to the new values of the axial mass introducing the muon mass effect gives predictions similar to the discrepancy between data and MC for MiniBooNE.

III.3 Fitting the modification

In order to use predictions for modified RS model we fitted the ratio of new models and RS for channels 3 and 5 as function of generated Q^2. Obtained functions were used to reweight the cocktail Monte Carlo. In figure 18 the top row shows the generated Q^2 distributions for RS model and its extensions separately for channels 3 and 5. In next three rows the fit to the ratio of new model to RS model for chanels 3 and 5 is shown.

In figure 19 data is compared with the Monte Carlo predictions for the RS model and its extensions. One can see the cross section suppression for the low Q^2 for new models. The BRS model together with new norm of the axial-vector form factor reduces the discrepancy from 35% to 20% and it is covered by the systematic uncertainties.

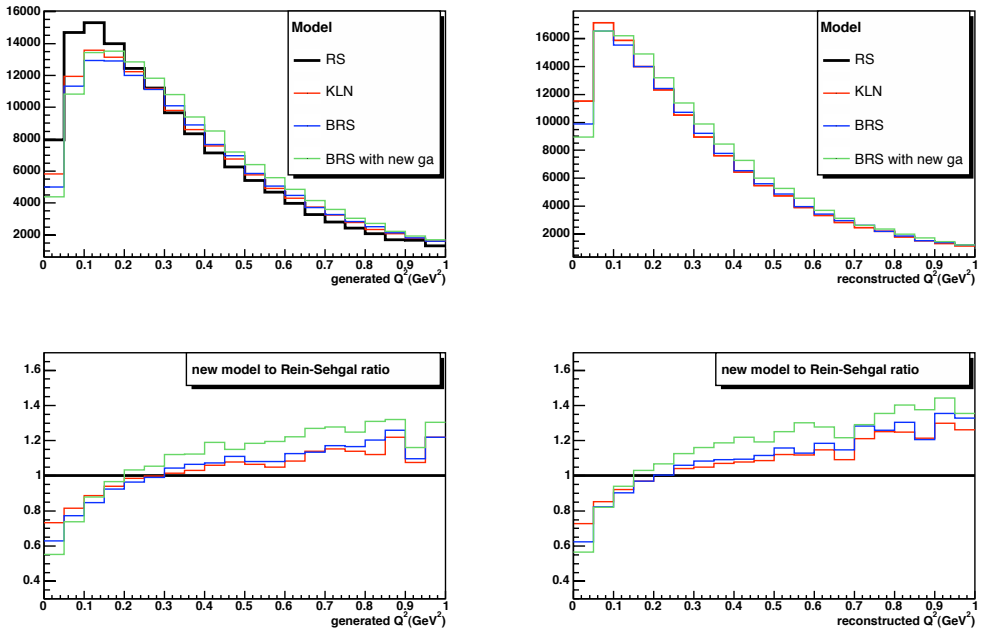

Figure 16: Nuance predictions for modified KLN model, BRS model, and BRS model with axial vector form factor from the Hernandez et al. In bottom the ratio of predictions for new models to predictions for the default RS model.

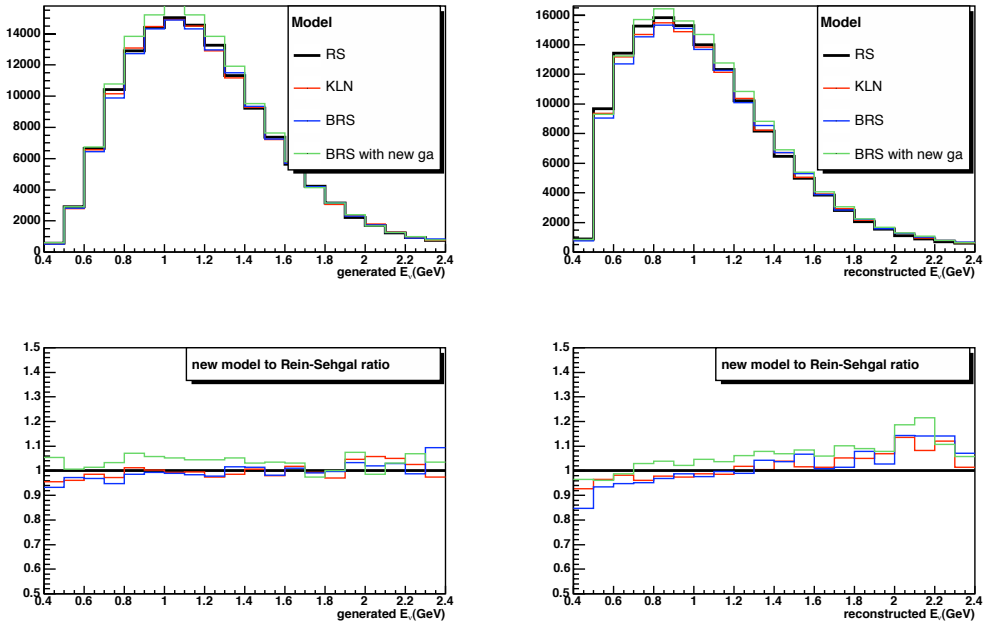

Figure 17: Nuance predictions for modified KLN model, BRS model, and BRS model with axial vector form factor from the Hernandez et al. In bottom the ratio of predictions for new models to predictions for the default RS model.

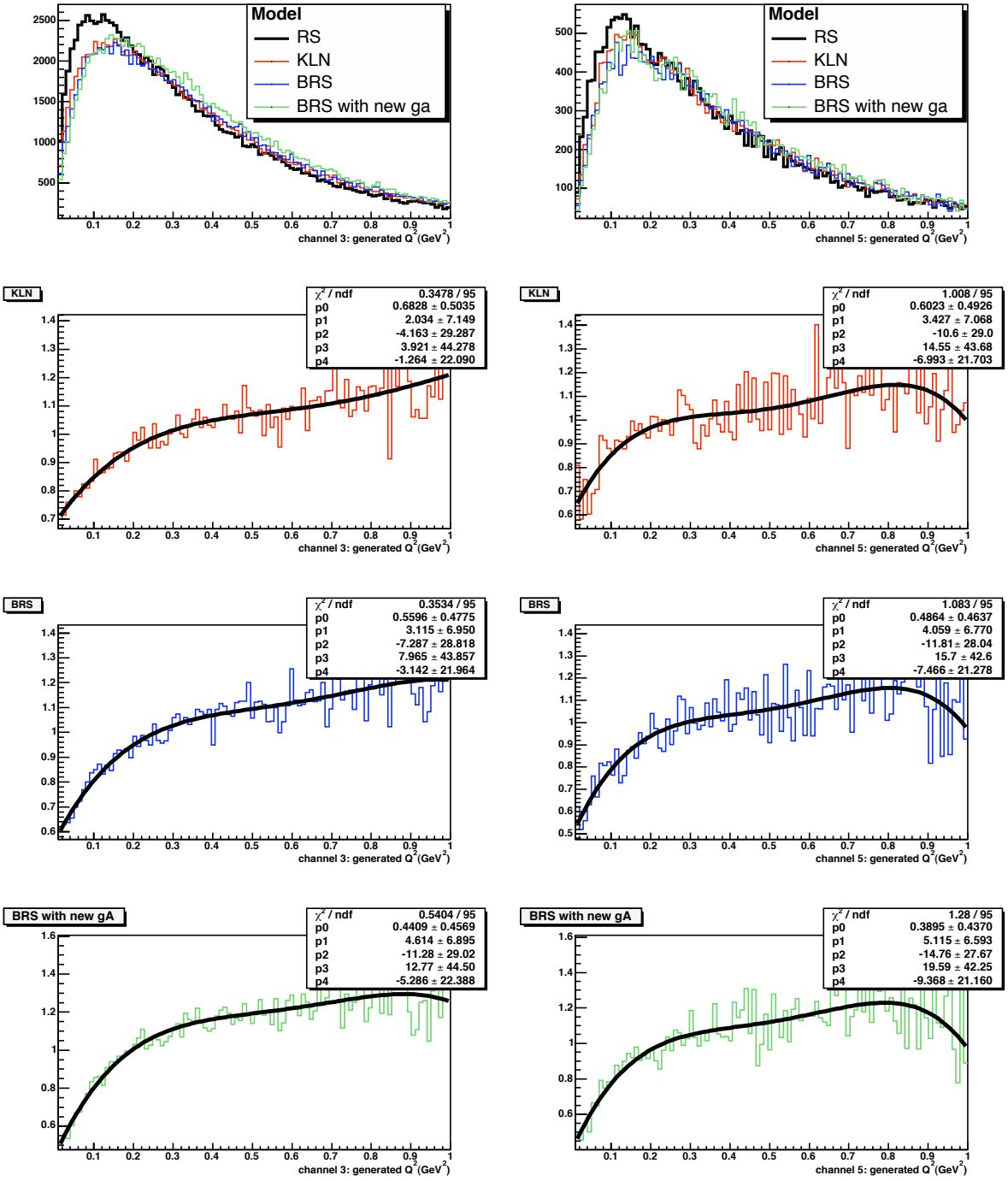

Figure 18: In the top row the generated Q^2 distributions for RS model and its extensions separately for channels 3 and 5. In next rows the fit to the ratio of new model to RS model for chanels 3 (left) and 5(right) is shown.

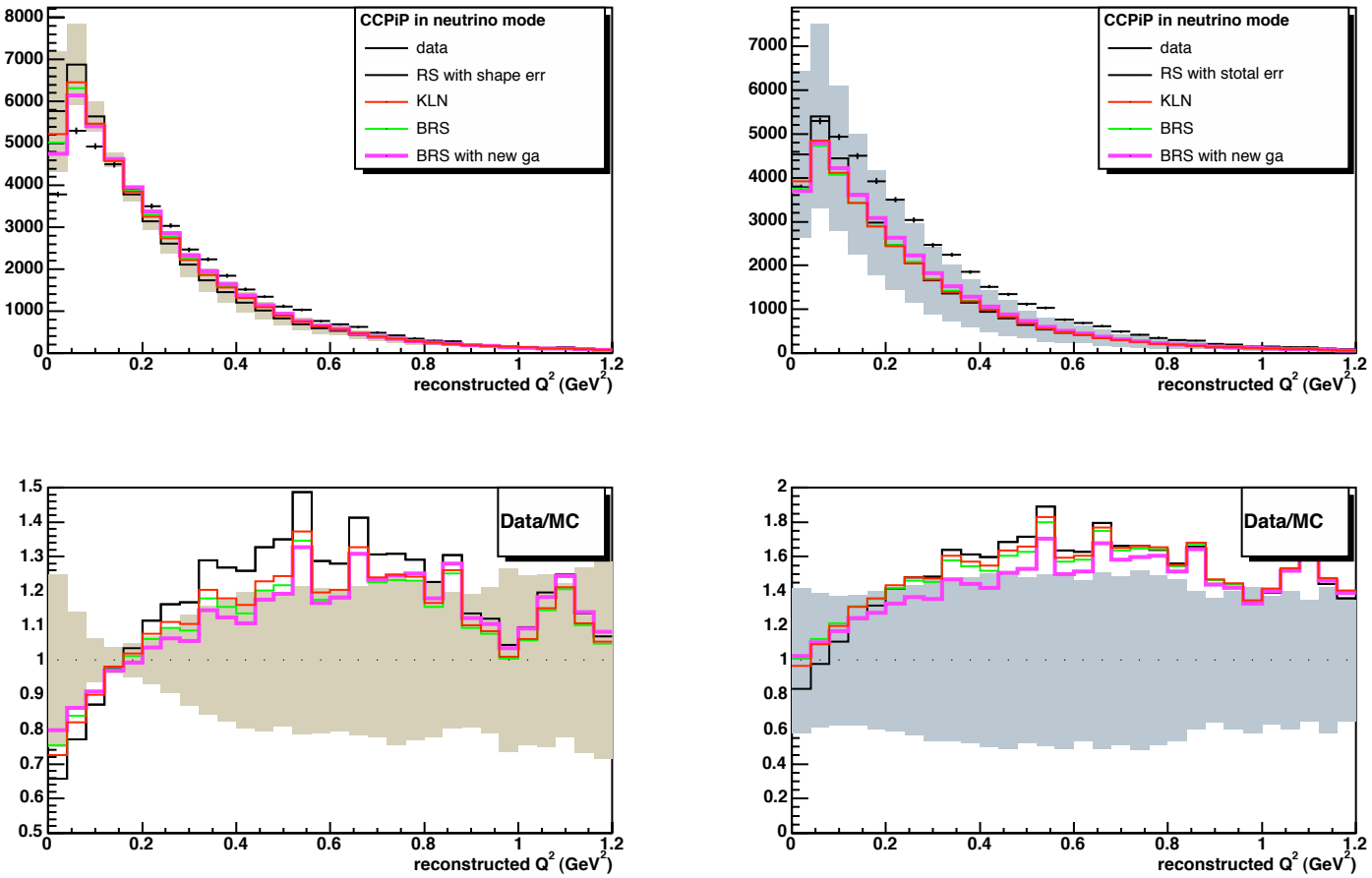

Figure 19: Data compared with the Monte Carlo predictions for the RS model and its extensions. In left column the relative normalization is shown while in right column the absolute one.

IV Adler screening in the coherent π^+ production

The neutrino scattering in the forward direction is described by the Adler PCAC theorem [19]. The inelastic charged current reaction

$$\nu_\mu + A \rightarrow \mu^- + F \tag{112}$$

where A is a nucleus and F denotes an inelastic channel, the cross section, neglecting the muon mass, is

$$\left(\frac{d\sigma}{dxdy}\right)_{PCAC} = \frac{G^2 ME}{\pi^2} f_\pi^2 (1-y)\sigma(\pi^+ + A \rightarrow F)\Big|_{E_\pi = Ey} \tag{113}$$

where $x = Q^2/2m\nu$ and the $y = \nu/E$, and ν again is the energy transfer and E the neutrino energy. The pion decay constant has the value $f_\pi = 0.93 m_\pi$. The extrapolation of the PCAC formula to non-forward angles is given by a slowy varying form-factor $\left[\frac{M_A^2}{M_A^2+Q^2}\right]^2$ with $M_A \approx 1GeV$. So the cross section has a following form

$$\frac{d\sigma}{dxdydt} = \frac{G^2}{4\pi^2} f_\pi^2 \frac{1-y}{y} A^2 \frac{1}{16\pi} \left[\sigma_{tot}^{\pi^+\mathcal{N}}(E_\pi = Ey)\right]^2 (1+r^2) \left(\frac{M_A^2}{M_A^2+Q^2}\right)^2 e^{-b|t|} F_{abs}(E_\pi = Ey) \tag{114}$$

$|t| = |(p_\pi - q)^2| = (\mathbf{p}-\mathbf{q})^\mathbf{2}$, A is a number of nucleons in the nucleus, b is related to nuclear radius R by

$$b = \frac{1}{3}R^2, \qquad (R = R_0 A^{1/3}), \tag{115}$$

and F_{abs} is a t-independent attenuation factor representing the pion absorption in the nucleus.

The important modification of the cross section is due to the muon mass. The modification can be found in the paper by Adler [20] and can be expresed as a simple multiplicative correction factor

$$\mathcal{C} = \left(1 - \frac{1}{2}\frac{Q_{min}^2}{Q^2+m_\pi^2}\right)^2 + \frac{1}{4} y \frac{Q_{min}^2 (Q^2 - Q_{min}^2)}{(Q^2+m_\pi^2)^2} \tag{116}$$

where

$$Q_{min}^2 = m_l^2 \frac{y}{1-y}, \qquad Q_{min}^2 \leq Q^2 \leq 2MEy_{max} \tag{117}$$

where $y_{min} = m_\pi/E$ and $y_{max} = 1 - m_l/E$.

Rein and Sehgal showed [23] that for the neutrino energy $E_\nu = 1.3GeV$ the suppression factor is $\mathcal{C}_{coh} \approx 0.75$. In the same paper the value for average screening factor for resonance model was presented $\mathcal{C}_{res} \approx 0.85 - 0.90$. The screening factor was applied only to the scalar part of the cross section (the S form factor in the equation 37) [24].

Figure 20 shows the comparison of the Rein-Sehgal model for coherent production with and without the Adler's screening factor and the fit to their ratio. In figure 21 data is compared with

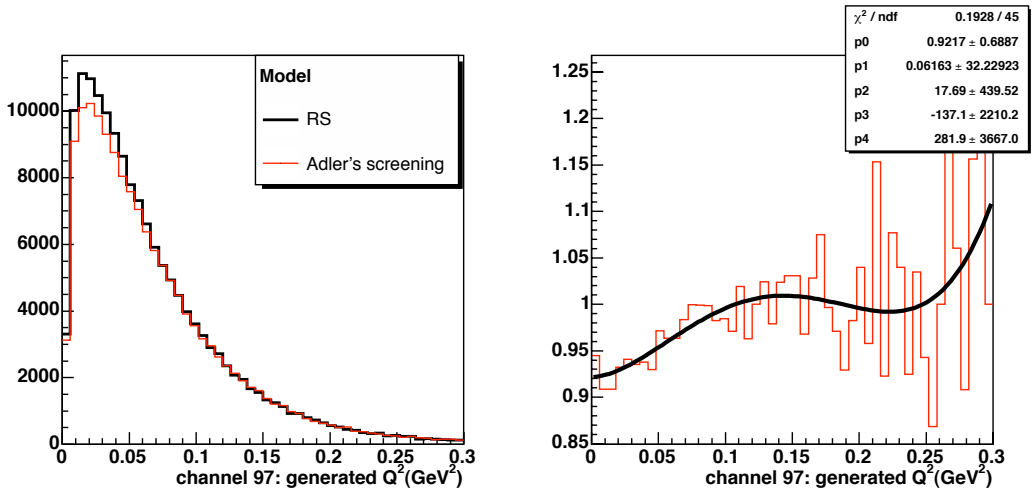

Figure 20: The coherent production for the Rein-Sehgal model with and without the Adler's screening (left figure). On the right side the fit to the ration of the both case is shown.

the Monte Carlo predictions for the RS and BRS models and BRS models with modified coherent contribution. The coherent production is modified for the muon mass effect (COH with muon mass), reduced to the half of the original contribution (COH/2) and removed from the sample (no COH). In left column the relative normalization is shown while in right column the absolute one. The muon mass effect does not change the distribution significantly because the coherent part is only about 6% on the $CC\pi^+$ sample. However, the smaller fraction of the coherent production in the $CC\pi^+$ sample is if *favorable*. The reduction to the half of coherent production reduces the discrepancy to about 10% only.

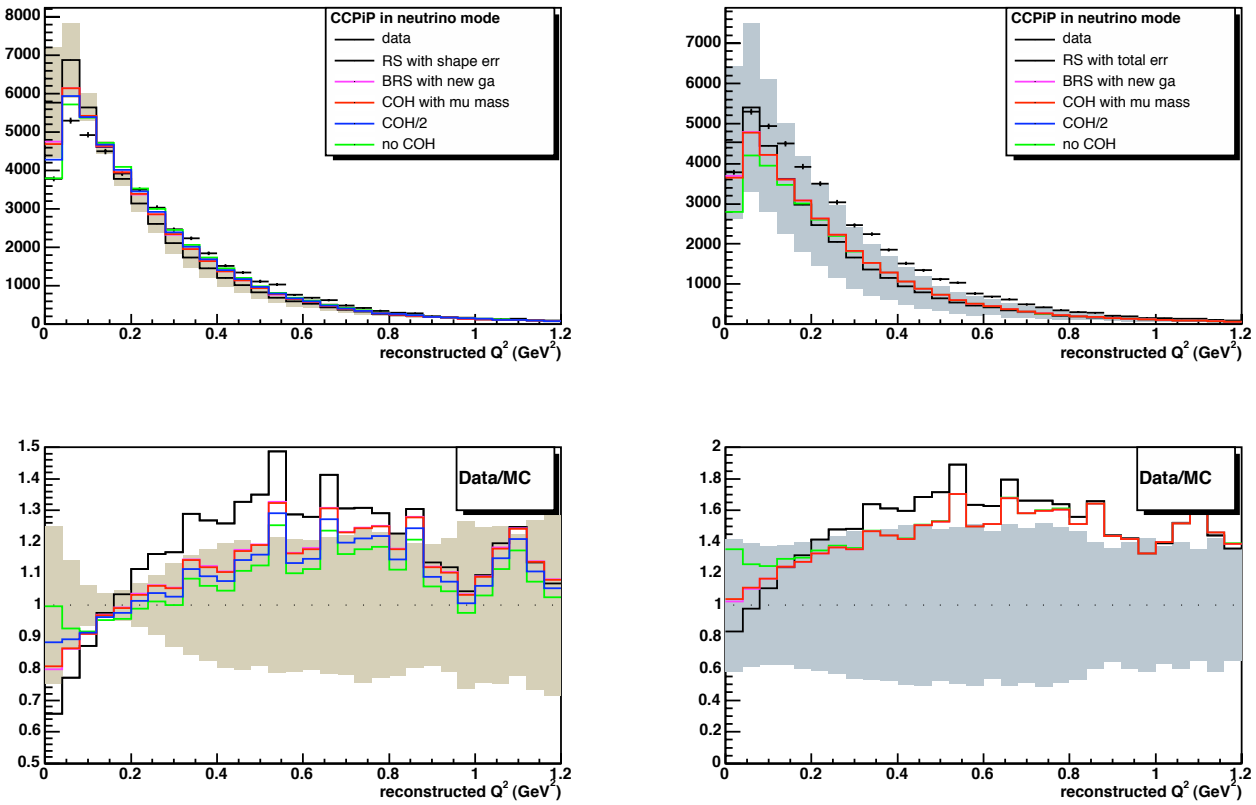

Figure 21: Data compared with the Monte Carlo predictions for the RS and BRS models and BRS models with modified coherent contribution. The coherent production is modified for the muon mass effect(COH with muon mass), reduced to the half of the original contribution (COH/2) and removed from the sample (no COH). In left column the relative normalization is shown while in right column the absolute one.

V X-Factor

The modification of the cross section changes the predicted number of events. We check the modification of the X-Factor after introducing new models. We used

- 5000 files from may_07_2_cocktail_new
- $POT_{MC} = 2.7425E21$
- $(N^{cc\pi^+}/POT)_{data} = 8.318E-17$

In table 3 the X-Factor for models discussed in previous sections is summarized. The difference between RS model and BRS model with new axial form factor is only about 1%, and removing coherent production results in increase the value of the X-Factor of about 9%.

Table 3: The X-Factor for models discussed in the technote.

1		$N^{cc\pi^+}$	$(N^{cc\pi^+}POT)_{MC}$	X-Factor
2	Rein-Sehgal	179597	6.55E-17	1.27
3	KLN	171276	6.24E-17	1.33
4	BRS	170745	6.23E-17	1.34
5	BRS and new g_A	177909	6.48E-17	1.28
6	5+ muon mass in coh	177545	6.45E-17	1.28
7	5 + coh/2	172903	6.31E-17	1.32
8	5 + no coh	167898	6.12E-17	1.36

VI Q^2 rescaling

The introduction of the muon mass to our model is an obvious step, but it explains only part of the low Q^2 discrepancy. Another possible explanation is that the muon energy distribution in the data is softer than in MC. To check it we rescaled the reconstructed Q^2. In figure 22 data is compared with the Monte Carlo predictions for reconstructed Q^2 rescaled by a factor given in the legend. One can see that rescaling reconstructed Q^2 by a factor greater than 1 reduced the discrepancy. Also the cross section for high Q^2 is reduced.

In figure 23 data is compared with the Monte Carlo predictions for the RS and BRS models and rescaled reconstructed Q^2 by factor 1.15. The combined BRS model with new axial-vector form

factor with rescaling reconstructed Q^2 gives extremely good prediction. Eventhough the combined results are with agreement with the observed distributions, there is no satisfying justification for the rescaling.

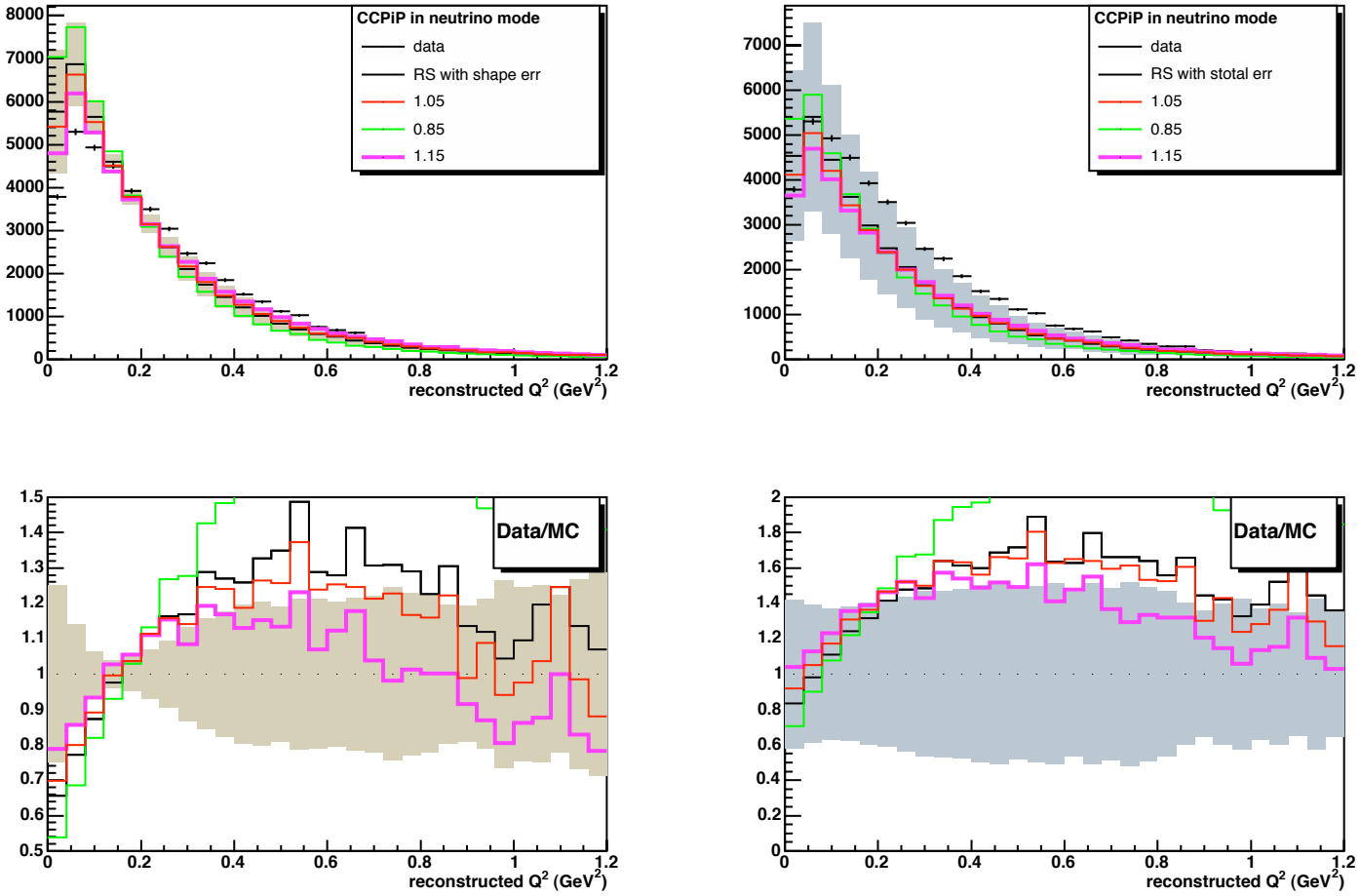

Figure 22: Data compared with the Monte Carlo predictions for reconstructed Q^2 rescaled by a factor given in the legend. In left column the relative normalization is shown while in right column the absolute one.

VII Summary

1. Taking into account the muon mass effect is essential.

2. The modification of axial vector form factor is necessary as well.

3. The Graczyk and Sobczyk model should confirm the predictions of Berger and Sehgal model

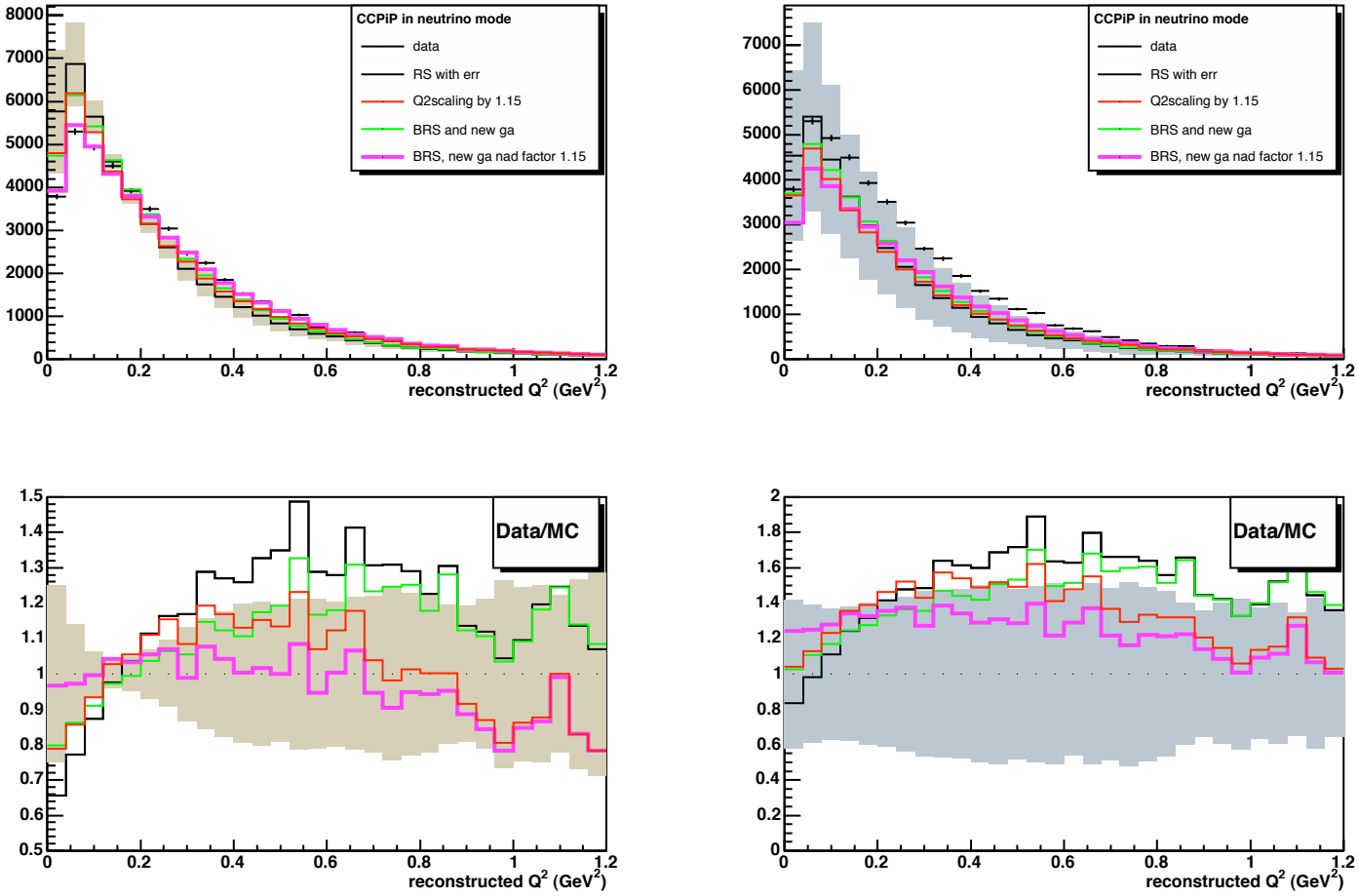

Figure 23: Data compared with the Monte Carlo predictions for the RS and BRS models and rescaled reconstructed Q^2 by factor 1.15. In left column the relative normalization is shown while in right column the absolute one.

(BRS).

4. The X-Factor dependence on modifications does not exceed 10%.

5. Adler's screening for the coherent $CC\pi^+$ production only slightly modifies prediction for the entire $CC\pi^+$ sample

6. The small coherent contribution is favorable

7. Next step: use the reweighting package (5 parameters for the axial vector form factor, muon mass model and vector form factor) to implement model for $CC\pi^+$ production.

8. Next^2 step: use different different values of the axial mass for free and bound nucleons.

9. Double check the reconstruction effect

References

[TN219] T. Katori, R. Tayloe, G. Zeller, "Update on the MiniBooNE numu QE Analysis"

[TN244] W. Metcalf, J. Nowak, S. Ouedraogo, "CCpi+ Sample in the Neutrino and Anti Neutrino Modes"

[1] A. A. Aguilar-Arevalo *et al.* [MiniBooNE Collaboration], "Measurement of muon neutrino quasi-elastic scattering on carbon," Phys. Rev. Lett. **100**, 032301 (2008) [arXiv:0706.0926 [hep-ex]].

[2] G. L. Fogli and G. Nardulli, Nucl. Phys. B **160** (1979) 116.

[3] R. P. Feynman, M. Kislinger and F. Ravndal, "Current Matrix Elements From A Relativistic Quark Model," Phys. Rev. D **3**, 2706 (1971)

[4] F. Ravndal, "Electroproduction of nucleon resonances in a relativistic quark model," Phys. Rev. D **4**, 1466 (1971).

[5] F. Ravndal, "Weak Production Of Nuclear Resonances In A Relativistic Quark Model," Nuovo Cim. A **18**, 385 (1973).

[6] K. M. Graczyk and J. T. Sobczyk,"Form Factors in the Quark Resonance Model," arXiv:0707.3561 [hep-ph].

[7] M. Hasegawa *et al.* [K2K Collaboration],"Search for coherent charged pion production in neutrino carbon interactions," Phys. Rev. Lett. **95**, 252301 (2005) [arXiv:hep-ex/0506008].

[8] D. Rein and L. M. Sehgal, "Neutrino Excitation Of Baryon Resonances And Single Pion Production," Annals Phys. **133**, 79 (1981).

[9] D. Rein,"Angular Distribution In Neutrino Induced Single Pion Production Processes," Z. Phys. C **35**, 43 (1987).

[10] O. Lalakulich, E. A. Paschos and G. Piranishvili,"Resonance production by neutrinos: The second resonance region," Phys. Rev. D **74**, 014009 (2006)

[11] O. Lalakulich and E. A. Paschos, "Resonance production by neutrinos. I: J = 3/2 resonances," Phys. Rev. D **71**, 074003 (2005)

[12] E. Hernandez, J. Nieves and M. Valverde,"Weak pion production off the nucleon," Phys. Rev. D **76**, 033005 (2007) [arXiv:hep-ph/0701149].

[13] F. Ravndal, "Weak Production Of Nuclear Resonances In A Relativistic Quark Model," Nuovo Cim. A **18**, 385 (1973).

[14] F. Rvndal, "Electroproduction of Nucleaon Resonances in a Relativistic Quark Model," Phys. Rev. D **4**, 1466 (1971).

[15] K. S. Kuzmin, V. V. Lyubushkin and V. A. Naumov, "Lepton polarization in neutrino nucleon interactions," Mod. Phys. Lett. A **19**, 2815 (2004) [Phys. Part. Nucl. **35**, S133 (2004)].

[16] C. Berger and L. M. Sehgal, "Lepton Mass Effects in Single Pion Production by Neutrinos," Phys. Rev. D **76**, 113004 (2007)

[17] C. Berger and L. M. Sehgal, "Erratum: Lepton Mass Effects in Single Pion Production by Neutrinos," Phys. Rev. D **77**, 059901(E) (2007)

[18] K. M. Graczyk and J. T. Sobczyk, "Lepton mass effects in weak CC single pion production," arXiv:0709.4634 [hep-ph].

[19] S. L. Adler, "Axial vector vertex in spinor electrodynamics," Phys. Rev. **177**, 2426 (1969).

[20] S. L. Adler,"Adventures in theoretical physics: Selected papers of Stephen L. Adler," arXiv:hep-ph/0505177.

[21] G. M. Radecky *et al.*, "Study Of Single Pion Production By Weak Charged Currents In Low-Energy Neutrino D Interactions," Phys. Rev. D **25**, 1161 (1982) [Erratum-ibid. D **26**, 3297 (1982)].

[22] T. Kitagaki *et al.*, "Study Of Neutrino D → Mu- P P(S) And Neutrino D → Mu- Delta++ (1232) N(S) Using The Bnl 7-Foot Deuterium Filled Bubble Chamber," Phys. Rev. D **42**, 1331 (1990).

[23] D. Rein and L. M. Sehgal,"PCAC and the Deficit of Forward Muons in π^+ Production by Neutrinos," Phys. Lett. B **657**, 207 (2007)

[24] L. M. Sehgal, private communication.